Earth-Science Reviews 127 (2013) 30–47

Contents lists available at ScienceDirect

Earth-Science Reviews

journal homepage: www.elsevier.com/locate/earscirev

Structural interpretation of the great earthquakes of the last millennium in the central Himalaya

J.-L. Mugnier [a,*], A. Gajurel [a,b], P. Huyghe [a], R. Jayangondaperumal [c], F. Jouanne [a], B. Upreti [b]

[a] ISTerre, Université de Savoie, CNRS, Université Joseph Fourier, Batiment les Belledonnes, Université de Savoie, F-73376, Le Bourget du Lac Cedex, France
[b] Department of Geology, Tribhuvan University, Ghantaghar, Kathmandu, Nepal
[c] Wadia Institute of Himalayan Geology, Dehradun, Uttarakhand, India

ARTICLE INFO

Article history:
Received 18 May 2012
Accepted 10 September 2013
Available online 19 September 2013

Keywords:
Paleo-seismology
Himalaya
Earthquakes
Quaternary sediment
Seismic hazard

ABSTRACT

A major question about the Himalaya remains open: does a great earthquake (like the Mw ~ 8.1 1934 earthquake) release all the strain stored by the Tibet–India convergence during the preceding interseismic period and only that strain, or can it also release a background store of energy that remained unreleased through one or more earlier earthquakes and so potentially engender giant events or a relatively random sequence of events? To consider this question, the history of the great earthquakes of the last millennium is investigated here by combining data provided by the historical archives of Kathmandu, trenches through surface ruptures, isoseismal damage mapping, seismites, and the instrumental record. In the Kathmandu basin, the location of the epicenter of the 1934 earthquake was determined from the arrival of high-energy P-waves that caused sedimentary dikes and ground fractures perpendicular to the epicenter azimuth. The epicenter of the Mw ~ 7.6 1833 earthquake can therefore be determined analogously from dike orientation, and its location to the NE of Kathmandu indicates an overlap with the Mw ~ 8.1 1934 rupture. The 1934 earthquake released strain not released by the 1833 earthquake.

Comparison of the historical records of earthquakes in Kathmandu with ^{14}C ages from paleo-seismic trenches along the Himalayan front suggests that: (1) the 1344 Kathmandu event ruptured the surface as far away as Kumaon and was therefore a giant Mw ≥ 8.6 earthquake; and (2) the 1255 event that destroyed Kathmandu is attested by surface ruptures in central and western Nepal and by seismites in soft sediment as far away as Kumaon. Geometric and rheologic controls for the different types of ruptures during the medium (Mw ~ 7), great (Mw ≥ 8), and giant (Mw > 8.4) earthquakes are illustrated in structural cross-sections. It is found that the epicenters of great Himalayan earthquakes are located on the basal thrust farther north or close to the locked zone, which is defined from geodetic measurements of regional deformation during the interseismic period; this suggests that great earthquakes initiate in a wide transition zone between exclusively brittle and exclusively creeping regimes, the extent of which depends on the dip of the Main Himalayan Thrust.

The succession of the great earthquakes during the last millennium has released all the 20-m millennial Himalayan convergence; even in the central seismic gap which has been locked since 1505, the millennial seismic release rate is close to the convergence rate. Nonetheless, no evidence of a succession of characteristic earthquakes has been found: the ~1100, 1833, and 1934 earthquakes in the eastern Himalaya are characterized neither by constant displacement nor by constant recurrence. Furthermore, some great earthquakes do not release all the strain elastically stored by the Himalayan and Tibetan upper crust: after the 1255 event, there was still the potential for a slip of several meters for the Mw ~ 8.1 1505 event. This suggests a rather random release of seismic energy; great earthquakes could occur anytime and in any part of the central Himalaya. Furthermore, a future giant earthquake of Mw ≥ 8.6 cannot be excluded.

© 2013 Elsevier B.V. All rights reserved.

Contents

* Corresponding author. Tel.: +33 4 79 75 86 76.
E-mail address: jean-louis.mugnier@univ-savoie.fr (J.-L. Mugnier).

0012-8252/$ – see front matter © 2013 Elsevier B.V. All rights reserved.
http://dx.doi.org/10.1016/j.earscirev.2013.09.003

1. Introduction

The present-day structure of the Himalaya results from progressive underthrusting of the Indian lithosphere along the Main Himalayan Thrust (MHT) beneath the Tibetan Plateau (Argand, 1924; Zhao et al., 1993) and great earthquakes of magnitudes >8 (Fig. 1) have episodically ruptured segments of the brittle upper part of the MHT several hundred kilometers long (Chandra, 1992). Historical archives of the great Himalayan city zone in the Kathmandu Valley indicate that several earthquakes of damage intensity >X have occurred during the last millennium (Chitrakar and Pandey, 1986; Pant, 2002; Mugnier et al., 2011). A seismic cycle is suggested by numerous studies based on geological and geophysical data (e.g. Molnar and Lyon-Caen, 1988) and by reconciliation of the long-term Holocene motion along the MHT (Lavé and Avouac, 2000; Mugnier et al., 2004) with its present-day inactivity, which can be inferred from GPS measurements (Bilham et al., 1997; Jouanne et al., 2004; Ader et al., 2012). The brittle upper part of the MHT is usually locked but sometimes ruptures producing great earthquakes (Avouac et al., 2001); this is a great threat to communities as it is only a matter of time until the next great earthquake happens in this densely populated area where many hydroelectric dams have been built. In any case, several questions remain open: (1) does a great earthquake (Mw > 8) release all the strain stored by the Tibet–India convergence during the preceding interseismic period, or (2) does it only release a portion of the stored energy, or (3) can it release all the energy not released during one or more preceding earthquakes (Feldl and Bilham, 2006)? In the first case, it would be possible to infer a rather regular seismic cycle, but in the other two cases, the background-stored energy would drive a more random or clustered sequence of events. Furthermore, in the second case, and as observed after the 2005 Kashmir earthquake (Jouanne et al., 2011), significant postseismic deformation might occur, and in the third case, giant earthquakes (Mw ≥ 8.4) cannot be excluded.

In order to answer these questions, interactions between convergence, seismic dynamics, and structural evolution have been considered. A succession of earthquakes in the central Himalaya is detailed in this paper from a compilation of the results obtained from seismite studies (e.g. Mugnier et al., 2011), trenching studies (e.g. Kumahara and Jayangondaperumal, 2012), historical archives (e.g. Pant, 2002; Ambraseys and Douglas, 2004) and the instrumental record (e.g. Chen and Molnar, 1977). In order to further specify the location of the 1833 earthquake, a study was developed to link the orientation of dikes affecting Quaternary sediments of the Kathmandu basin with the characteristics of earthquake shaking. Three structural cross-sections were constructed in order to discuss the effect on the extent of great earthquake ruptures of (1) inherited structures, (2) lateral variation in along-strike segmentation of the MHT, and (3) the extent of the transition zone between purely brittle and purely creeping regimes.

These sections allow us to specify the extent and geometric variability of the ruptures, the regularity of the seismic cycle, and the inferred minimum earthquake magnitudes in the Himalaya.

2. Seismo-tectonic setting of the central Himalaya

2.1. Structure of the Himalaya

The Himalaya is formed by a stack of thrust sheets (Le Fort, 1975). Two major thrusts (from north to south, the Main Central Thrust (MCT) and Main Boundary Thrust (MBT)) are presently passively displaced above the basal Main Himalayan Thrust (MHT) and respectively form the southern limits of the High Himalaya and Lesser Himalaya domains; the Lesser Himalaya domain thrusts over the Siwalik Hills (or Outer Himalaya). The MHT absorbs about 20 mm/yr of convergence in Nepal, which is nearly half of the present convergence between India and Eurasia (Bilham et al., 1997; Bettinelli et al., 2006; Mugnier and Huyghe, 2006). It is locally imaged by geophysical data (Zhao et al., 1993; Avouac, 2003; Schulte-Pelkum et al., 2005) and a crustal ramp has been deduced from balanced cross-sections and indirect models which associate: (1) the clustering of micro-seismicity with stress increase in the vicinity of the ramp (Pandey et al., 1995); (2) the increase in topography and fluvial incision with increasing dip of the MHT (Lavé and Avouac, 2001); (3) the present-day velocity field with the mechanical behavior of the crust in the vicinity of the ramp (Berger et al., 2004); and (4) the thermo-chronological data with thermo-kinematic models (Robert et al., 2011).

The combination of all these approaches indicates a geometry of the MHT (e.g. Schelling and Arita, 1991), which is characterized by a southern frontal ramp (Main Frontal Thrust (MFT)), a detachment

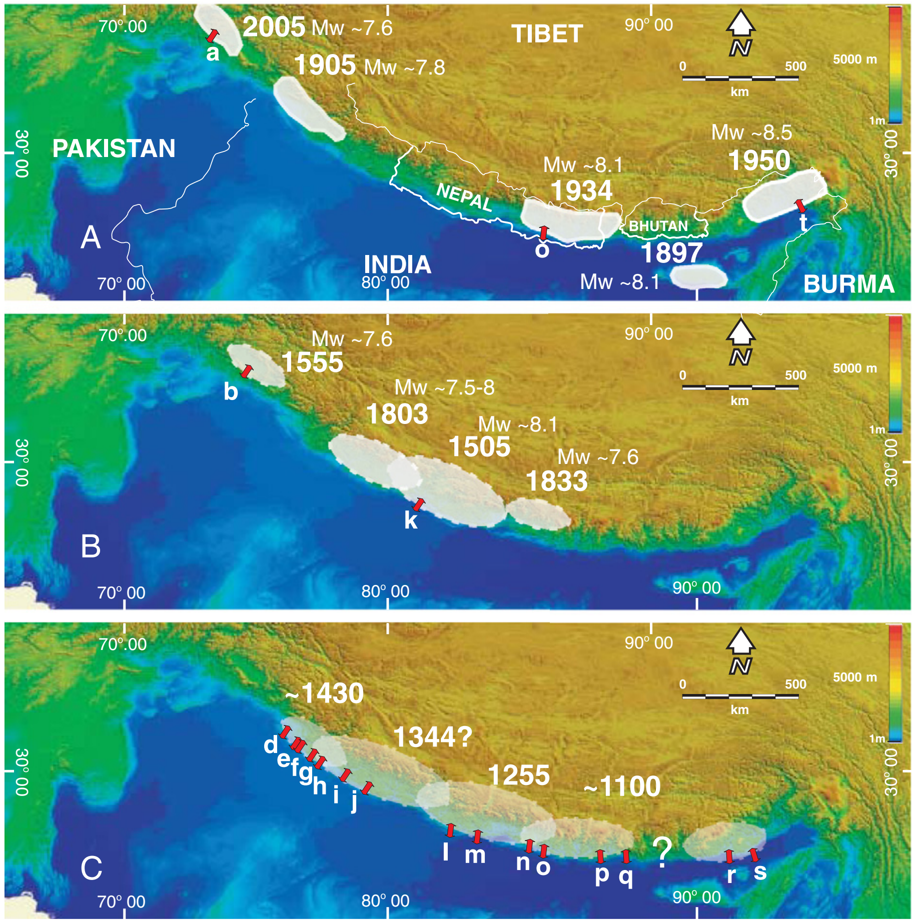

Fig. 1. The great earthquakes of the last millennium in the Himalaya. A) The 1897, 1905, 1934, 1950 and 2005 earthquakes are defined by instrumental data and surface damage (e.g. Bilham et al., 2001; Avouac et al., 2006); B) from 1890 to 1500, the great earthquakes are mainly defined from surface damage (e.g. Ambraseys and Jackson, 2003; Ambraseys and Douglas, 2004); C) from 1500 to 1000 they are mainly defined from fault strands exposed in trenches. The red arrows refer to the main trenches at the front of Himalaya and are indicated at the front of the inferred ruptures: (a) Muzaffarabad site (Kondo et al. (2008); (b) Riasi site (Vassallo et al., 2012); (c) Hajipur site (Malik et al., 2010); (d) Bhatpur (Kumahara and Jayangondaperumal, 2012); (e) Chandigarh (Malik et al., 2008); (f) Chandigarh (Kumar et al., 2006); (g) Kala Amb (Kumar et al., 2001); (h) Rampur Ganda (Kumar et al., 2006); (i) Lal Dang and (j) Ramnagar (Kumar et al., 2006); (k) Mohana Khola (Yule et al., 2006); (l) Koilabas Khola (Mugnier et al., 2006); (m) Bandelpokhari (Upreti et al., 2008); (n) Marha Khola (Lavé et al., 2005); (o) Sir Khola (Sapkota et al., 2013); (p) Hokse (Nakata et al., 1998); (q) Chalsa (Kumar et al., 2010); (r) Nameri (Kumar et al., 2010); (s) Harmutty (Kumar et al., 2010); (t) Marbong (Jayangondaperumal et al., 2011).

beneath the Outer and Lesser Himalaya, a crustal ramp cutting through the crust of the Indian plate, and a lower ramp flat that extends far to the north beneath the Tibetan Plateau (Fig. 2). Furthermore, the dip of the MHT as well as the location and size of the crustal ramp vary laterally along strike: the ramp is located at a depth of ~10–18 km beneath the MCT surface trace in central Nepal and at a depth of ~8–15 km to the south of the MCT in western Nepal (Pandey et al., 1999; Berger et al., 2004; Mugnier et al., 2011; Robert et al., 2011).

2.2. Seismic cycle in the Himalaya

GPS measurements of the present-day deformation field (Banerjee and Burgmann, 2002; Jouanne et al., 2004) suggest that, during the interseismic period, thrust displacement occurs in the deeper, ductile northern part of the MHT only. No slow earthquakes have been detected in GPS time series recently (Bettinelli et al., 2006; Ader et al., 2012) in the brittle, external locked part of the MHT (Fig. 2B and C). The creeping zone is usually modeled as a dislocation that extends to the trailing edge of the locked zone (Bilham et al., 1997), although a zone of transitional rheology (brittle creeping from Marone, 1998) is defined by Berger et al. (2004) between the locked and regularly creeping zones.

Aseismic slip during the interseismic period induces stress accumulation at the southern edge of this shear zone, which triggers intense microseismic activity and elastic strain in the upper crust at the front of the high range (Pandey et al., 1995). The elastic deformation is released, in the long term, by major earthquakes occurring along the fault plane of the MHT (e.g. Avouac, 2003). Their hypocenters are close to the stress accumulation zone at the brittle–ductile transition and the ruptures propagate toward the Indian plain along the MHT (e.g. Avouac et al., 2001). Some of these ruptures reach the surface at the front (e.g. Mugnier et al., 1992), causing fault scarps (e.g. Kumar et al., 2010) or fault-related folds (e.g. Champel et al., 2002), while others reach the surface along out-of-sequence thrusts (Huyghe and Mugnier, 1992; Mugnier et al., 2005), as with the 2005 (Mw ~ 7.6) Kashmir earthquake (Avouac et al., 2006; Kaneda et al., 2008). Not every earthquake, however, reaches the surface, such as the instrumentally-detected 1991 (Mw ~ 6.8) Uttarkashi event (Cotton et al., 1996) or the 1905 (Mw ~ 7.8) Kangra event (Molnar, 1987), both of which were located west of the studied zone.

The extent of ruptures at depth is usually poorly known and the instrumentally measured 1991 Uttarkashi event provides some of the most robust data on the connection between seismic source and structural geology in the Himalaya. Its hypocenter was located from inversion of accelerograms at a depth of 14 (+1/−4) km and the fault plane had a dip of 11 (+3/−6)° (Cotton et al., 1996). The rupture initiated close to the locked line defined by Banerjee and Burgmann (2002) and propagated mainly toward the SW (Cotton et al., 1996). This gently dipping event occurred along the lower flat of the MHT inferred by

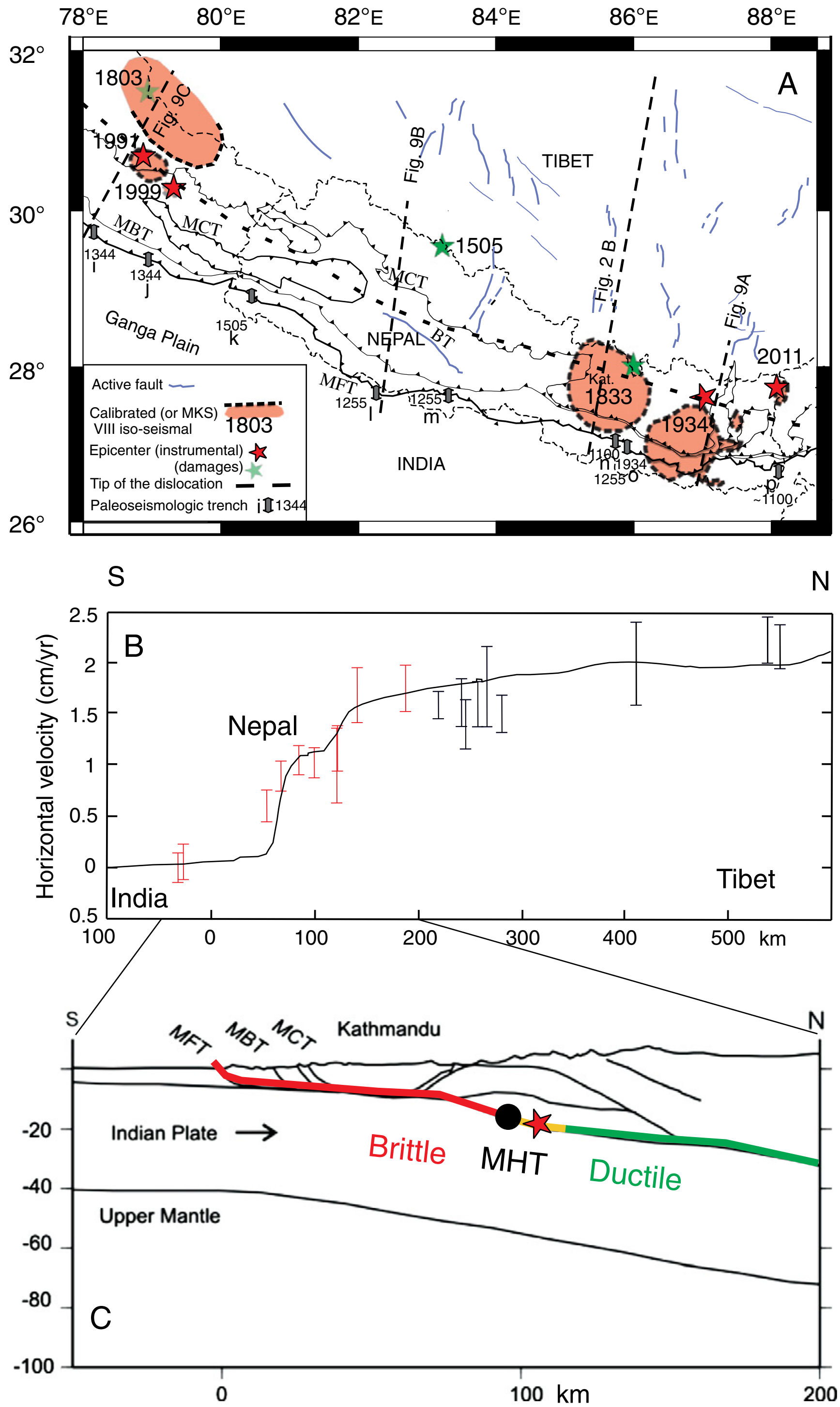

Fig. 2. A) Structural map of the Himalaya of Nepal and Kumaon–Garhwal. Calibrated isoseismal contours for Intensity = VIII from Ambraseys and Douglas (2004) for the 1934, 1803, and 1833 events and MMI intensity from Rastogi and Chadha (1995) for 1991 event and from USGS (2011) for 2011 event. Instrumental location of 1934 epicenter from Chen and Molnar (1977), 1991 epicenter from Rastogi and Chadha (1995) and from USGS (2011) for 2011 event. References of trenches (h) to (p) are indicated on the caption of Fig. 1 and interpretation of the age of the paleoseismic events is from Fig. 4C. B) Horizontal shortening in Himalaya and Tibet during interseismic periods. Data are from Zhang et al. (2004). The continuous line refers to the elastic–plastic modeling of Berger et al. (2004), suggesting a shear rate of 21 mm/yr along the MHT beneath central Tibet. C) Schematic cross-section through central Nepal (from Lavé and Avouac, 2000); the red and yellow bars, black dot, and red star are respectively the inferred rupture zone, the transition zone between ductile and brittle regimes (from Berger et al., 2004), the tip of dislocation (from Bettinelli et al. (2006), and the hypocenter of great earthquakes (from Avouac et al., 2001).

Srivastava and Mitra (1994) and most of the associated zones of severe damage intensities (up to VIII) were located south of the epicenter (Rastogi and Chadha, 1995; Fig. 2A).

The lateral extent of great earthquake ruptures is probably controlled by structural complexities (Wesnousky, 2008) that trend obliquely to the Himalayan chain. For example, Molnar (1987) and Hough et al. (2005) showed the role of lateral ramps in the segmentation of the 1905 earthquake into several domains, and Mugnier et al. (2011) suggest that a lateral ramp bounded the 1934 earthquake in the vicinity of Kathmandu. The 2011 event (Mw 6.9) at the Nepal/Sikkim border

(USGS, 2011) may also have occurred along a lateral ramp of the MHT because it was related to a slip motion from the strike at a shallow level (10–30 km) that did not affect the surface.

Moderate earthquakes (4 < Mw < 7) frequently occur along a portion of the MHT or along steeper out-of-sequence thrusts. The 1999 Chamoli earthquake (Satyabala and Bilham, 2006) exemplifies such an out-of-sequence event along a fault that dips ~15° northwards, and is steeper and shallower (10 ± 3 km) than the MHT.

2.3. Great earthquakes revealed by trenches

Numerous trenches have been excavated along the MFT since 1998 in order to study the paleoseismic events that ruptured the surface. Fig. 3 provides a synopsis of these trenches (Nakata et al., 1998; Upreti et al., 2000; Kumar et al., 2001; Lavé et al., 2005; Kumar et al., 2006; Yule et al., 2006; Malik et al., 2008; Upreti et al., 2008; Kondo et al., 2008; Kumar et al., 2010; Mugnier et al., 2011; Jayangondaperumal et al., 2011; Vassallo et al., 2012; Kumahara and Jayangondaperumal, 2012; Sapkota et al., 2013). An interpretation, mainly based on Lavé et al. (2005) and Kumar et al. (2006) suggests two giant earthquakes occurred (Feldl and Bilham, 2006) at ~1100 in eastern Nepal and at ~1400 in the northwestern Himalaya, which respectively produced more than 14 m and 18 m slip (Fig. 3B). Nonetheless, the lateral correlations between ruptures—and their temporal relationships—revealed in the different trenches are debated and the slip values are highly dependent on the structural models used for trench interpretation (Jayangondaperumal et al., 2013). In eastern Nepal, trench orientation and the strike of the thrusts strikes are very oblique to the Himalayan shortening direction; only a 10 m slip is found (Supplementary Discussion S2 of Lavé et al., 2005) while using a slip partitioning model for conversion of vertical offset into slip value along the Himalayan slip vector direction; additionally, the thrust component may be enhanced by the rotation of slip direction which is evidenced in the vicinity of lateral ramps (Mugnier et al., 1999). In the northwestern Himalaya, Kumar et al. (2006) estimated the slip from the dip of the faults and the height of the scarp, but the former is observed locally only, whereas the latter records multiple events. From new trenches and re-interpretation of data from previous trenches, Kumahara and Jayangondaperumal (2012) report two distinct events: one after 1400 for the western segment and one before 1400 for the eastern segment. Furthermore, Jayangondaperumal et al. (2013) suggest that the highest scarp related to the pre-1400 event (Rampur Ghanda scarp) also records an older event. Therefore at least three events seem to be recorded in the trenches of the northwestern Himalaya.

An alternative scenario for the great earthquakes of the last millennium (Fig. 3C) is therefore proposed in the following sections based on a combination of the analysis of seismites, historical archives, and results from trenching studies.

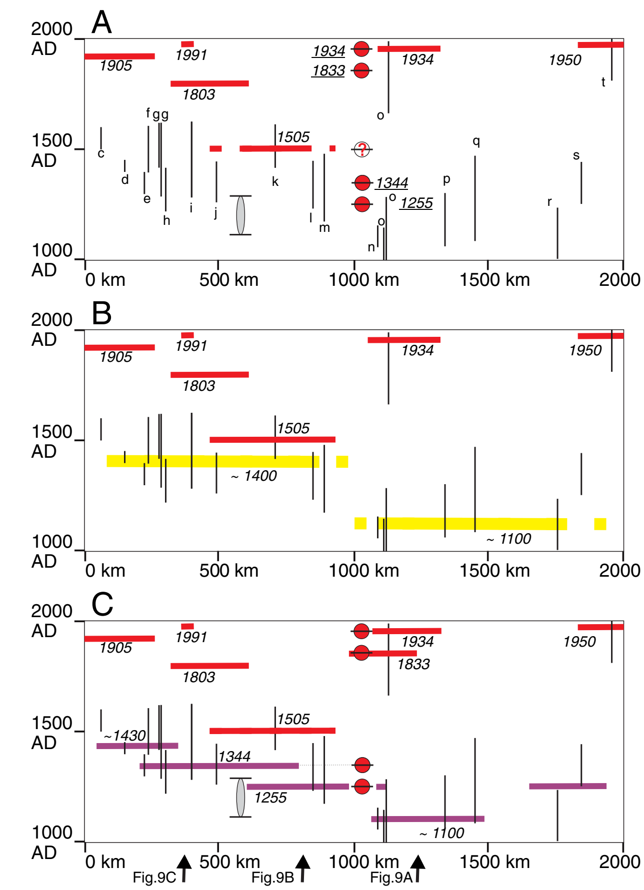

Fig. 3. Space–time diagram showing dating constraints for the timing of surface displacements at trenching sites along the Himalaya front. A — Data. The horizontal scale is the along-arc distance; References and location of trenches (a) to (t) are indicated in Fig. 1, the vertical bars above each site reflect the time range of surface displacement allowed by dating in calendar years. The red horizontal bars refer to the historical earthquakes determined from iso-seismal studies (Ambraseys and Douglas, 2004) or rupture modeling (Cotton et al., 1996). The red dots refer to great intensity events in Kathmandu (Pant, 2002). The dot with a question mark refers to the 1505 event not quoted in Kathmandu. The gray ellipse refers to seismites (Rajendran and Rajendran, 2011). B — The yellow horizontal bars refer to the interpretation of two giant earthquakes (adapted from Kumar et al., 2010); C — the purple horizontal bars refer to our interpretation of great earthquakes, adapted from Mugnier et al. (2011) and Kumahara and Jayangondaperumal (2012), and based on the integration of the historical archives of Kathmandu and seismites in a Himalayan structural framework.

3. Historical earthquakes and seismites in the Kathmandu Valley

Kathmandu is the largest city in the Himalaya and the valley in which it is located lies above the locked segment of the MHT (Fig. 2). The basin within the valley is filled with a very thick (500–600 m) sequence of Pliocene to Pleistocene fluvio-lacustrine sediments (Yoshida and Igarashi, 1984). Drainage of the corresponding paleo-lake was initiated ~10000 yr ago through headward erosion of the Bagmati River and was followed by incision of the basin (Gajurel, 2006).

Lacustrine sediments and environments are prone to the development of fractures, dikes, and soft-sediment deformation related to in situ deformation during earthquake shaking (Mugnier et al., 2011). Furthermore, the effect of the thick soft-sediment filling at the site and the quality of the historical archives make the Kathmandu basin one of the best archives from which to develop a calendar of historical earthquakes in the central Himalaya.

3.1. Great earthquakes in the Kathmandu Valley

Kathmandu has a long history of destructive earthquakes. At least 10 major earthquakes (Chitrakar and Pandey, 1986; Pant, 2002; Mugnier et al., 2011) feature in historical records since the 13th century (Table 1).

The quality of archives has greatly improved since the 18th century, meaning the magnitude of great Himalayan earthquakes can be calibrated (Ambraseys and Douglas, 2004). For this period, the biggest earthquakes in the Kathmandu basin occurred in 1934 (Mw 8.1) and 1833 (Mw 7.6).

3.1.1. The 1934 event

The 1934 earthquake induced strong shaking of eastern Nepal and the Bihar plain. Rana (1935) and Dunn et al. (1939) report damage that approached Modified Mercalli Intensity X (Fig. 4). The 1934 earthquake killed 20% of the population and damaged 40% of all buildings in the Kathmandu Valley (Pandey and Molnar, 1988).

Table 1

Great earthquakes in central Himalaya; the row number in column (*) are used in Fig. 10; length and slip (**) provided from methods indicated in Section 4.2.1); the number of trench (***) refers to the sites (labeled a to q on Figs. 1 and 2) that are considered to be affected by the event; No, H, S and In respectively for trench, historical, seismological and InSAR studies. In italic: results inferred from an indirect model or not very reliable data. In addition to the main reference listed on the left and right side, the following references are used: [1]Chitrakar and Pandey (1986); [2]Bilham (2004); [3]this paper, [4]Ambraseys and Douglas (2004); [5]Levi et al. (2006); and [6]Feldl and Bilham (2006).

Historical record				Event characteristics				Trench studies				
(*)	Main reference	Date (AD)	MM intensity in Kathmandu	Length km (**)	Slip m (**)	Magnitude Mw	Location	Number of trenches (***)	Name	Reference Trench Surface slip (m)	^{14}C age (CalAD)	Main publication
1)	No historic record	~1100	*>X[a]?*	280–400	9–18	*~8.8[5]* *~8.6[3]*	Eastern Nepal	4 (n,o,p,q)	Marha Khola (n)	17	>1160 <1020	Lavé et al. (2005)
2)	H Pant (2002)	1255 (06/07)	>X	300–400	6–12	*≥8.1[a3]*	Central Nepal	3 (l,m,o)	Koilabas Khola (l)	8	>1442 <1224	Mugnier et al. (2011)
3)	H Pant (2002) *Or 1408 AD[1]*	1344 (09/14)	*>X* X[1]	300–500	13–16	*≥8.4–9.2[6]*	Kumaon (India)	5 (e,g,h,i,j)	Rampur Ghanda (h)	16	>1422 <1222	Kumar et al. (2006)
4)	No historic record	~1430		160–200	7–9	*8.2[3]*	Himachal (India)	3 (d,f,g)	Bhatpur (d)	9	>1400–<1460	Jayangondaperumal et al. (2013)
5)	H Ambraseys and Douglas (2004)	1505 (06/06)	*≥VII[b]?*	250–400	9–18	*8.1[4]*	N29.50° E83.00°	1 (k)	Mohana Khola (k)	18	>1610 <1410	Yule et al. (2006)
6)	H Ambraseys and Douglas (2004)	1803 (09/01)	*≥IV[b]*	100–200	3–5	7.5[4] 8[2]	N31.50° E79.00°			None		
7)	H Bilham (1995)	1833 (08/26)	X	50–70	2–4	7.6[4]	N28.00°[3] E86.00°[3]			None		
8)	H, S Chen and Molnar (1977).	1934 (01/15)	>X	160–250	2–5	8.1[4]	N27.55° E 87.09°	1 (o)	Sir Khola (o)	3	<1630	Sapkota et al. (2013)
9)	S India Meteorology. Dep.	1991 (05/23)	III	42–48	0.6–0.8	7.0	N30.75° E78.86°			None		
10)	S, In Satyabala and Bilham (2006)	1999 (03/28)	II			6.2	N30.44° E79.39°			None		
	S: USGS (2011)	2011 (09/18)	V			6.9	N 27.72° E 88.06°			None		

[a] From comparison with 1934 AD event.
[b] Not quoted in the archive and deduced from distance/damage attenuation relationship of Ambraseys and Douglas (2004).

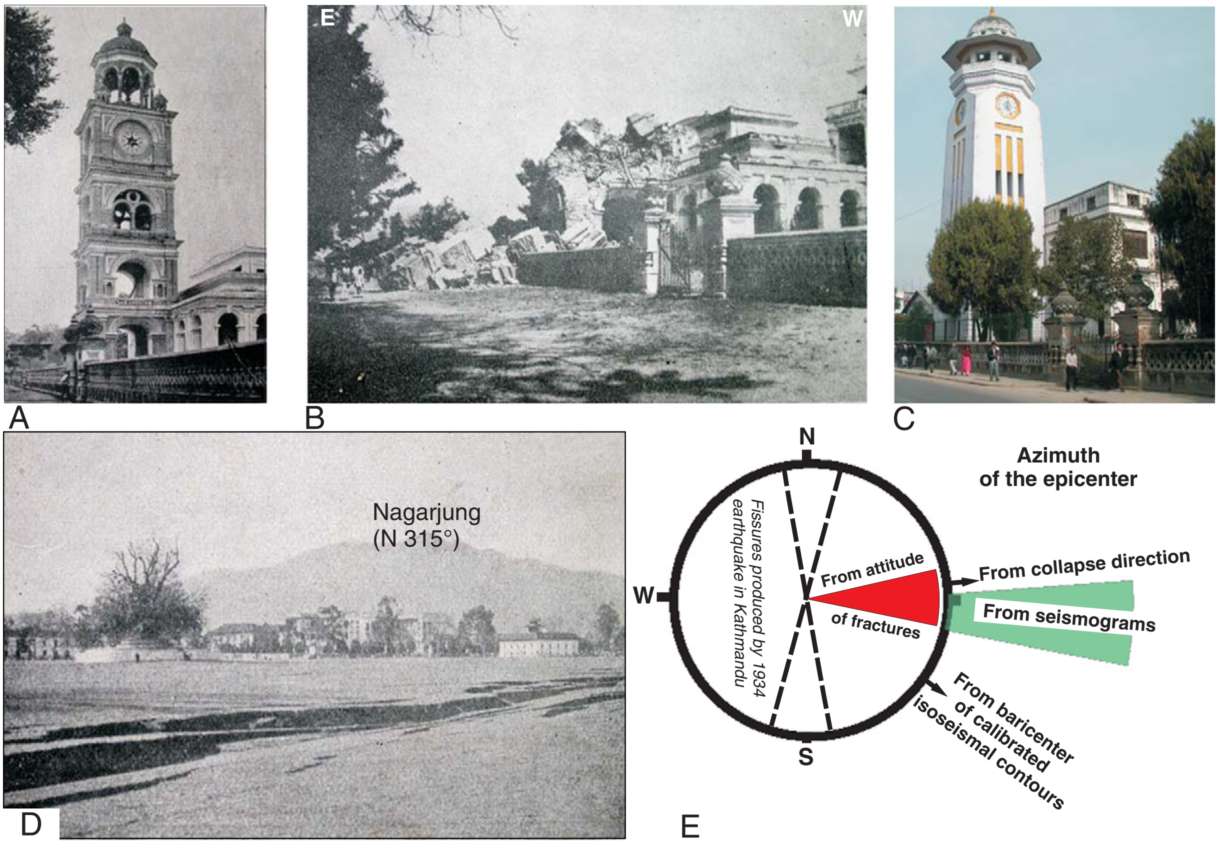

Fig. 4. Surface effects of the 1934 earthquake in Kathmandu: A) Clock Tower before destruction (photograph from Rana, 1935); B) Clock Tower collapsed N265E (photograph from Dunn et al., 1939); C) modern Clock Tower (2000); D) surface fractures at Tudikhel due to the earthquake, looking N315E (photograph from Rana, 1935), E) comparison between the azimuth of the epicenter deduced from seismograms of three seismic stations (Chen and Molnar, 1977); the direction of collapse (panel B and Dunn et al., 1939), the barycenter of calibrated isoseismal contours (Ambraseys and Douglas, 2004) and the normal to the 1934 fractures at Tudikhel.

3.1.1.1. The epicenter of the 1934 earthquake. The location of the 1934 epicenter has been a point of contention due to the absence of an unambiguous surface rupture (Dunn et al., 1939), scarcity of information in the Tibet area, and occurrence of amplification effects at various sites that increased destruction in the alluvial plain (Pandey and Molnar, 1988). The isoseismal maps of Ambraseys and Douglas (2004) indicate a barycenter of maximum intensity to the E–SE of Kathmandu (Fig. 4E). The proposed epicenter location has therefore varied from beneath the Ganga plain (Dunn et al., 1939) to beneath the High Himalaya (from instrumental seismicity of Chen and Molnar, 1977; Fig. 2); the supposed location of the epicenter ~170 km east of Kathmandu is nonetheless based on just three seismic stations and the uncertainty of its determination is greater than 30 km. Recent trenching demonstrates that an ~3 m surface rupture affected the MFT during the 1934 earthquake (Sapkota et al., 2013). It is therefore suggested that the 1934 event ruptured the entire locked zone of the MHT (Sapkota, 2011) and that the epicenter was located at the northern boundary of the calibrated damage intensity VIII zone.

3.1.1.2. Damage and ground deformation associated with the 1934 earthquake. Damage in the Kathmandu Valley was studied by Rana (1935) and Dunn et al. (1939). The soft-sediment filling (Dixit et al., 1998) meant that damage was worse in the southern part of the basin (Fig. 5). Nonetheless, the effect of liquefaction was probably weak during the 1934 event, given that Dunn et al. (1939) reported that "subsidence of ground, and tilting and slumping of the houses were entirely absent". This interpretation is consistent with a geotechnical map of the Kathmandu Valley (HMG of Nepal, 1993) which indicates that a major liquefaction hazard is restricted to the zones of modern river terraces.

The details (especially the view angle and direction of damage) of certain photographs have been re-examined in this paper in order to characterize the trend of damage zones: the emblematic Clock Tower of Tri-Chandra College (Fig. 4A from Rana, 1935) was destroyed by the 1934 earthquake (Fig. 4B from Dunn et al., 1939) and rebuilt on the same base (Fig. 4C). The tower fell in a N265E direction, that is, obliquely to the walls of the square tower; the collapse of the tower was therefore determined by the dominant direction of shaking. Furthermore, other pillar structures (Pl. 24 of Dunn et al., 1939) and numerous objects (Pl. 4 of Dunn et al., 1939) fell in the same direction: for example, the nine-story "Dharahara" tower located near Tudikhel was broken at the fifth story and collapsed in the same direction as the Clock Tower (Photos in Kesharmahal Library, Kathmandu). Fractures observed in photos of the flat, central part of the valley were not related to lateral spreading because they were located far from the present-day river risers (Fig. 4D). Nonetheless, they still exhibit slight displacement with mainly dip slip motion; the perpendicular direction to these ground fractures was between N70°E and N85°E (Fig. 4E).

Therefore the collapsed pillars and towers indicate that the azimuth of the epicenter of the 1934 earthquake, which has been independently deduced from seismograms and the associated fractures, trended nearly perpendicularly to the dominant direction of shaking. This point is further discussed in Section 3.2.

3.1.2. The 1833 events

The main 1833 event was preceded by two foreshocks that drove people outdoors in alarm thus reducing loss of life. The main shock reached IX MM intensity in the Kathmandu area and up to X MM intensity in the southern part of the basin (Bilham, 1995; Fig. 5). The main

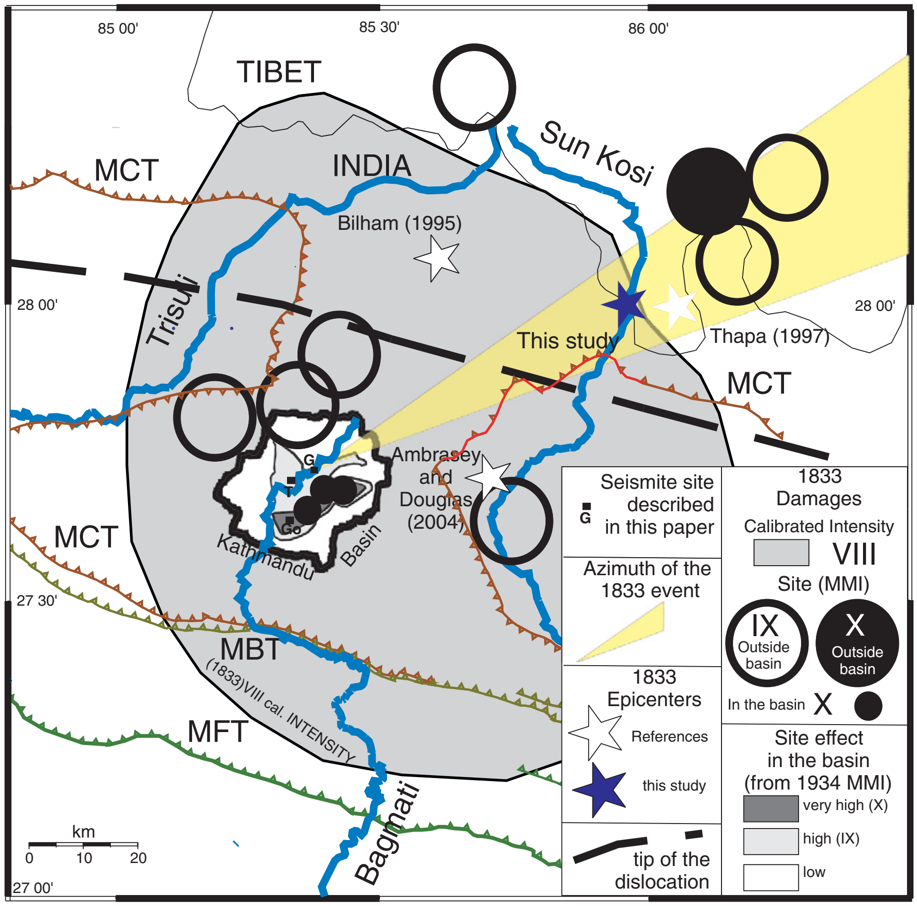

Fig. 5. Sketch of the Himalayan belt at the longitude of Kathmandu. IX and X MMI intensity distribution for sites of the 1833 earthquake from Bilham (1995). Calibrated intensities for the 1833 earthquake from Ambraseys and Douglas (2004). Tip of the dislocation (northern boundary of the locked zone) from Bettinelli et al. (2006). Black squares refer to the seismites described in this paper: Go (Godavari, Fig. 8); G (Gothatar, Fig. 6); T (Tudikhel, Fig. 4D). See text and Fig. 6 for the azimuth determination of the 1833 event. Amplification of damage by the site of the Kathmandu Valley is inferred from IX and X MMI intensity distribution for the 1934 earthquake (adapted from Dixit et al., 1998).

event was followed in the next months by two events of VIII–IX MM intensity (Bilham, 1995).

3.1.2.1. The epicenter of the 1833 earthquake. The main 1833 earthquake was recorded throughout the region from Tibet to the Ganga plain; it affected the Tibetan regions located north of Kathmandu very badly. Uncertainty about the epicenter location is in great part due to the lack of records from eastern Nepal, precluding any precise determination of the isoseismals. It has been successively proposed that the epicenter was located beneath the Ganga plain (Oldham, 1883), in western Nepal (Seeber and Armburster, 1981), or north/northeast (Bilham, 1995), northeast (Thapa, 1997) and east (Ambraseys and Douglas, 2004) of Kathmandu.

These different interpretations are discussed (Section 3.2.2) in light of the characteristics of the clastic dikes associated with the earthquake.

3.1.2.2. Clastic dykes coeval with the 1833 earthquake. At Gothatar village, on the left bank of the Bagmati River, unconsolidated Recent sediments were deformed (Fig. 6A). In the upper part, soft-sediment deformation affected a 30 cm-thick silt layer; in the lower part, three sand dikes cut through an undeformed layer (Fig. 6B and C). The dikes are connected to the coarse sand source layer below; they extend upward into the undeformed layer and their strikes vary between N150E and N165E (Fig. 6D). The dikes are oblique to both the NNE to SSW direction of the Bagmati River and local relief, and so did not originate by lateral spreading. ^{14}C dating of two charcoal samples recovered from the soft-sediment deformation layer (Mugnier et al., 2011) results in calibrated ages (Stuiver et al., 1998; Reimer et al., 2004) between 1812 and 1893, and between 1832 and 1883. We therefore propose that the soft-sediment deformation and dikes were formed during the 1833 seismic event (see discussion in Mugnier et al., 2011).

3.1.3. The oldest earthquakes

For the oldest earthquakes, the record is rather incomplete and the dates that appear in the historical archives are difficult to reconcile; for example, the event previously cited as 1408 by Chitrakar and Pandey (1986) may be the same as the 1344 event cited by Pant (2002) due to a revision of the calendar. Magnitudes and epicenter locations are conjectural and we propose in this paper to compare the historical record in Kathmandu with the ^{14}C dates of the great earthquakes found in trenches (Table 1) in order to precisely date the age of the ruptures in trenches and the location of historical earthquakes that damaged Kathmandu.

We hypothesize that the 1344 event in Kathmandu (Pant, 2002) is related to the surface rupture dated by ^{14}C at between 1278 and 1433 (Kumar et al., 2006) or between 1282 and 1422 (Kumahara and Jayangondaperumal, 2012) in Kumaon trenches. The regional extent of the severe damage intensity zone for the 14th century event is consistent with the giant earthquake interpretation of Feldl and Bilham (2006).

We suggest relating the 1255 event in Kathmandu (Pant, 2002) to the surface rupture dated by ^{14}C at between 1442 and 1224 in central Nepalese outcrops (Mugnier et al., 2005). This central Nepalese location would also explain the numerous liquefied sand layers and sand blow features (Fig. 7A) dated at 1111–1292 in soft sediment of the Kosi River terraces in Kumaon (Rajendran and Rajendran, 2011). Sapkota

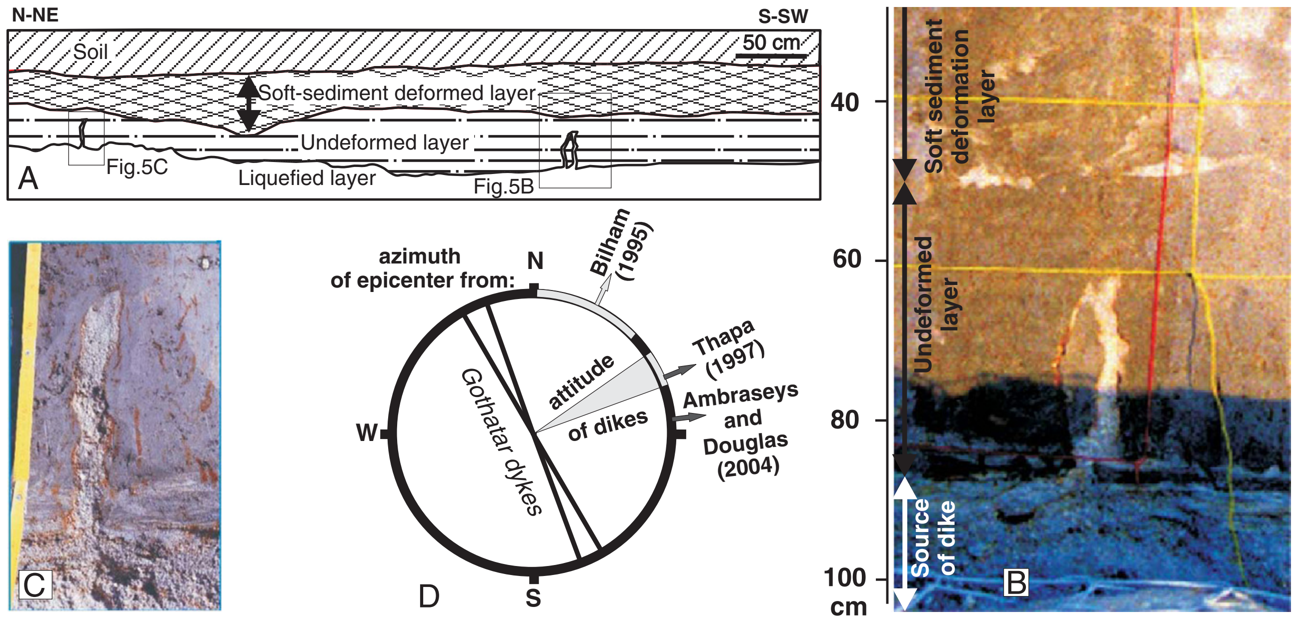

Fig. 6. Seismites in the sediments of the Bagmati River at Gothatar; A) Trench cross-section, with location of panels B and C; two charcoals were found within the soft-sediment deformation layer and yield respectively ages between 1812 and 1893 and between 1832 and 1883; B) section from top to source level, with a dike and a soft-sediment deformation level, C) detail of a dike; D) comparison between the orientation of the 1833 dikes and the azimuths of the epicenter respectively inferred by Bilham (1995), Thapa (1997), Ambraseys and Douglas (2004).

et al. (2013) also relate the 1255 event to the surface rupture ^{14}C-dated between 1300 and 700 in Sir Khola trench (eastern Nepal), although this time interval also includes the ~1100 event identified in the close Marha Khola trench by Lavé et al. (2005).

3.2. Dikes and epicenter location

Very few attempts have been made to link the orientation of paleo-liquefaction structures with the tectonic stress field (Obermeier et al., 2002); furthermore, the empirical observations of Obermeier (1996) suggest that dike orientation is mainly influenced by local relief and lateral spreading and only to a minor degree by the direction of shaking. We nonetheless suggest that the direction of shaking is relevant in the Kathmandu area, because the zones where fractures are observed are flat and no sedimentary levels were affected by widespread liquefaction (HMG, 1993).

Furthermore, earthquake-ground fractures provide a clue for inferring stress directions and earthquake locations (e.g. Ambraseys, 1988) and the example of crack orientation at the Andean plate margin (Loveless et al., 2009) clearly records a long-term distribution of seismic events.

However, the relationship between the trend of damage zones and seismic wave propagation is ambiguous. For example, two separate interpretations were proposed from the fall of tombstones during the 1933 Long Beach earthquake: Clements (1933) initially suggested that the damage zone trend was linked to waves moving in the vertical plane (P-waves) parallel to the azimuth of the epicenter but Benioff (1938), finally, ascribed it to shear (S) waves.

In the following discussion, dike development in the Kathmandu basin is briefly described and some basic seismic concepts are recalled in order to explain an empirical relationship that relates dike orientation to epicenter location in the case of well documented Himalayan earthquakes.

3.2.1. Geometry and timing of dikes and soft-sediment deformation in the Kathmandu basin

Soft-sediment deformation and the formation of clastic dikes in the Himalaya have recently been related to in situ deformation of sediments during earthquake shaking (Jayangondaperumal et al., 2008; Mugnier et al., 2011; Rajendran and Rajendran, 2011), and are thus considered to be seismites.

The soft-sediment deformation structures that develop close to the water/sediment interface and the narrow dikes are in fact two end members of seismites (Fig. 7B and C); the various geometries observed in the Kathmandu basin are due to the superposition of these two types of structures (Mugnier et al., 2011). The dikes of the Kathmandu area

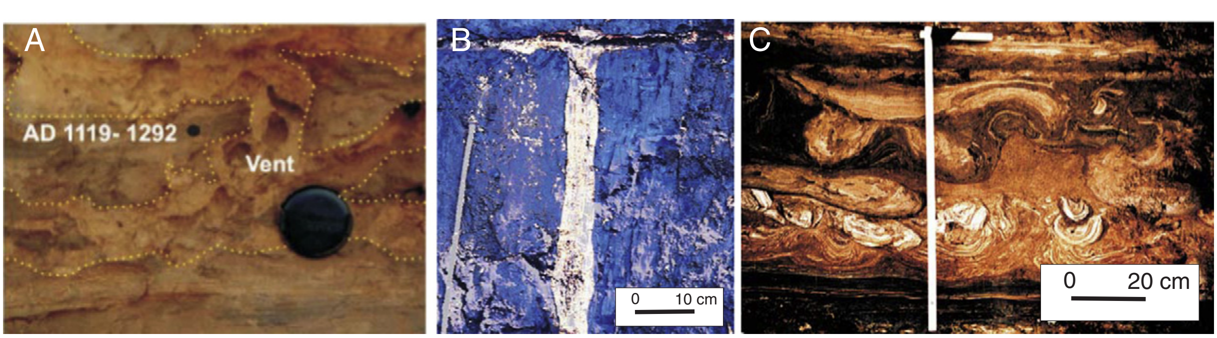

Fig. 7. Examples of seismites in the Himalaya; A) sandblow features (dotted outline) close to Almora (Kumaon, India), from Rajendran and Rajendran (2011); B) typical dike and sand cone at Chapagaon (Kathmandu valley); C) typical pillow structure at Thimi (Kathmandu Valley, from Mugnier et al., 2011).

differ slightly from those described by Obermeier (1996) in that no thick dikes and/or general liquefaction of sandy levels are found in the basin, while they differ from those described by Levi et al. (2006) in that they are of small vertical extent.

As an example, Fig. 8 illustrates the relative timing of the deformation that affected the initial layered sedimentary pile at Godawari (Mugnier et al., 2011): dike 1 developed (Fig. 8B); soft-sediment deformation in the upper level induced folding of dike 1 (Fig. 8C); dikes 2 and 2a cut through the soft-sediment deformation level (Fig. 8D); the liquefaction of the source bed occurred during the development of both dikes 1 and 2 (Fig. 8B and D) and was probably synchronous with the soft-sediment deformation that affected the upper level between the development of these dikes; dike 3 cut through the source layer of dikes 1 and 2 (Fig. 8E). On the time scale of the sedimentary record, all these deformations occurred simultaneously because all the cones lay upon the same paleo-surface; the development of the different structures fits with a single cause linked to a seismic event during which dike initiation predates soft-sediment deformation.

3.2.2. Strain field during earthquakes

At any site, in the initial earthquake stage, the first recorded waves are pressure waves, which induce deformation with a principal strain axis parallel to the direction of propagation and therefore parallel to the azimuth of the epicenter (e.g. Stein and Wysession, 2003). Shear waves propagate at a velocity less than $Vp/2^{1/2}$, where Vp is the velocity of the P-waves; the delay between P and S arrivals therefore increases with distance from the epicenter (e.g. Stein and Wysession, 2003). The P-wave energy decreases rapidly with distance (D) from the epicenter due to its body wave characteristics. However, close to the epicenter, and due to their high frequency, P-waves can induce destructive accelerations. The greatest motions usually occur later, associated with the arrival of the surface waves and with a complex pattern and temporal evolution of strain orientation.

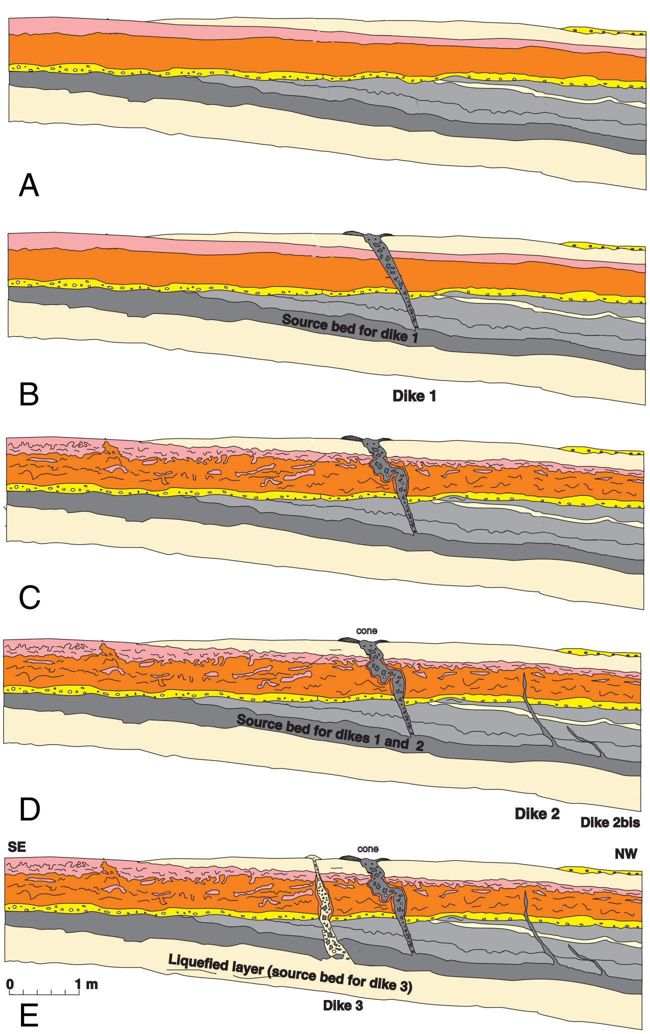

Fig. 8. A sketch of the development of dikes and soft-sediment deformation at Godawari (Kathmandu Valley); A) initial stage; B) after dike 1 development; C) after soft-sediment deformation; D) after dike 2 development; E) after dike 3 development.

Vp is 5.6 km/s for the Himalayan crust (Pandey et al., 1999) and Vs is less than 4 km/s. For the 1934 earthquake, the distance between Kathmandu and the epicenter was only 170 km meaning that the P waves were of high energy, whereas the delay between the P and S arrival was greater than 106 s. During this period, the Kathmandu Valley was strongly shaken and the P waves moved in the direction of the azimuth of the energy source, i.e. the zone whose rupture initiated the event; therefore, the ground fractures formed with a strike nearly perpendicular to the epicenter azimuth whereas the pillars fell nearly parallel to the azimuth of the epicenter.

Similar relationships were observed for the 2005 Kashmir event: the fractures in the floodplain near Jammu are tension fractures perpendicular to the azimuth of the epicenter (Jayangondaperumal et al., 2008) and the building destruction pattern located near and up to ~250 km away from the epicenter was compatible with motion in a plane parallel to the azimuth of the epicenter (Jayangondaperumal and Thakur, 2008).

These observations are compatible with an empirical interpretation of fractures that initiate upon the arrival of seismic waves. Nonetheless, such an interpretation is only valid when the co-seismic features are initiated by high-energy P-wave.

3.2.3. The location of the 1833 and 1934 events

We expect that the 1833 and 1934 seismic waves exhibit similarities because these two events were geographically close and linked to thrusting along the MHT. We therefore apply the same trend assumption to the dikes associated with the 1833 event and consider that they too strike perpendicular to the epicenter azimuth. The above empirical analysis of the damage associated with the 1934 earthquake (Section 3.1.1.2) and dikes related to the 1833 event (Section 3.1.2.2) allows us to refine the location of the 1833 epicenter with respect to the 1934 epicenter.

The orientation of earthquake-ground fractures suggests that the 1934 epicenter lay east of Kathmandu in the Himalayan belt (Fig. 4), in the northern part of the surrounding uncertainty zone defined by Chen and Molnar (1977). Assuming that clastic dikes formed in a plane perpendicular to the azimuth of the epicenter (see Section 4.1.2), we posit that the 1833 event was located northeast of Kathmandu. In addition, we suggest that the epicenter was located in the northeastern part of the zone of high damage intensity (Fig. 2), as with the 1991 and 1934 earthquakes. This proposed epicenter location is surrounded by sites of IX and X MM intensities (Fig. 5) (Campbell, 1833, reprinted in Bilham, 1995) and is close to the location proposed by Thapa (1997).

The 1934 event reached the MFT (Sapkota et al., 2013) and Feldl and Bilham (2006) estimated 8–9 m of slip at the epicenter.

The main 1833 event produced about 5–6 m of slip at the epicenter (Feldl and Bilham, 2006), although it did not rupture the surface (Dunn et al., 1939). The main shock (August 26) could have extended at depth to the northern part of the Kathmandu basin and could have been followed by strong aftershocks probably located close to or south of Kathmandu on October 4 and 18 (Mugnier et al., 2011).

The above adjustment of the 1833 and 1934 earthquake epicenters suggests that they were about 100 km apart. The 1934 shaking propagated 150 km from east to west (Bilham et al., 2001; Hough and Bilham, 2008) and therefore overlapped with the 1833 epicenter, confirming that an ~50 km common segment moved successively during these two events (Bilham, 2004).

4. Structural control of great earthquakes

4.1. Great earthquakes and the brittle/ductile transition zone beneath the Himalaya

The seismic model of the Himalaya (e.g. Avouac, 2003) is based on a model with brittle deformation in the upper crust and ductile deformation at deeper levels. Geological observation (Sibson, 1986), rate- and state-variable friction laws (Scholz, 1998), and mechanical models of long-term deformation (Shibazaki et al., 2002) provide evidence for a transition zone where deformation is accommodated by both brittle and plastic processes. At temperatures between 250 and 400 °C, rate strengthening is activated (e.g. Marone, 1998), which allows a brittle, creeping part of the fault between the brittle part ($0 < T < 250$ °C) and the ductile part ($T > 400$ °C). Such a domain involving brittle creep was clearly evidenced for the 1999 Taiwan (Perfettini and Avouac, 2004) and the 2005 Kashmir (Jouanne et al., 2011) thrust earthquakes, which nucleated in the shallower portion of the brittle/ductile transition zone and which were followed by post-seismic creep and clustering of small scale earthquakes along the deeper part of the thrusts.

Such a transition zone between brittle and plastic deformation is defined by Berger et al. (2004) for the MHT between the locked zone and the regularly creeping zone. The distribution of the epicenters of the great earthquakes along a zone perpendicular to the arc (Fig. 2) could possibly be linked to the projection of the intersection between the MHT and the isothermal zone associated with this brittle creeping rheology; this assumption is tested by projecting the epicenters along three structural cross-sections of the central Himalaya (Fig. 9).

Great uncertainty remains when determining epicenter locations from incomplete damage intensity descriptions: in the upper range of the scale, maximum damage intensity in any earthquake affecting vulnerable structures appears to be effectively the same; that is, the scale saturates at VII–VIII MSK intensities (Ambraseys and Douglas, 2004); quantitative methods of evaluating the remote damage attenuation in the lower range of the scale posit an ~120 km error for epicenter location (Szeliga et al., 2010). Therefore, we follow Ambraseys and Douglas (2004) and retain the epicenter location deduced from the barycenter of the VIII calibrated intensity zone absent any seismological or structural data with which to refine the damage distribution. This assumption usually furnishes a location to the south of the actual one, as is shown by comparison with the determination of the epicenter by instruments for the 1934 and 1991 events; it therefore minimizes the extent of the brittle zone along the MHT.

4.1.1. Great earthquakes in eastern Nepal

We draw a cross-section through the common portion of the 1833 and 1934 ruptures (Fig. 9A). The geometry of the thrust sheets is adapted from Schelling and Arita (1991) with addition of the Ramgarh Thrust of Pearson and DeCelles (2005); the location of the crustal ramp is inferred from the work of Lavé and Avouac (2001), Berger et al. (2004) and Schulte-Pelkum et al. (2005). In this cross-section, the geometric transition between the lower flat and the ramp is close to the tip of the dislocation (Bettinelli et al., 2006) and the brittle creeping zone is narrow (Berger et al., 2004). This suggests that nucleation of the 1934 and 1833 events occurred close to the lower flat/ramp transition (Avouac, 2003).

A rupture involving more than 14 m of surface displacement occurred in ~1100 affecting all of eastern Nepal (Nakata et al., 1998; Lavé et al., 2005). It is thought that this earthquake nucleated below the High Himalaya domain, that the rupture associated with this earthquake broke through the surface trace of the MFT, and reached Mw ~ 8.5 (Lavé et al., 2005).

Between the ~1100 earthquake and the 1833 events, several earthquakes affected Kathmandu, although the epicenters of the 1255, 1344, and 1505 earthquakes were probably located west of the city (Table 1) and the 1681, 1767, and 1810 events were minor compared to the earthquake in 1833. Therefore, the ~1100, 1833, and 1934 earthquakes (Pandey and Molnar, 1988) form a succession of great earthquakes along the MHT, which are not characterized by constant displacement or constant recurrence.

4.1.2. Great earthquakes in western Nepal

A regional structural cross-section through western Nepal (Fig. 9B) was adapted from Berger et al. (2004) and Mugnier et al. (2005) for the MHT geometry. The surface geology is adapted from Dhital and Kizaki (1987) for the outer Lesser Himalayan duplex, from Fuchs and Frank (1970) for the inner Lesser Himalayan duplex and from personal observations in this zone. Furthermore, several active faults are evidenced along this cross-section and were related to MCT or MBT reactivation, oblique-slip back-thrusting along the Bari Ghat fault (Nakata, 1989) and reactivation of faults in the Siwalik domain (Mugnier et al., 2005).

In western Nepal, two great earthquakes occurred in 1255 (Mugnier et al., 2011) and in 1505 (Ambraseys and Jackson, 2003). The 1255 event broke through the surface trace of the MFT in western Nepal (Mugnier et al., 2005, 2011), strongly shook Kathmandu, and was presumably the cause of surface damage and soft-sediment deformation in the central Himalaya ^{14}C-dated between 1292 and 1119 (Rajendran and Rajendran, 2011).

The epicentral area of the 1505 earthquake was in northwest Nepal and southwest Tibet and the greatest destruction occurred in Lo Mustang and Globo (Ambraseys and Douglas, 2004); therefore the epicenter was probably located in a very northerly position (Fig. 9B), close to or just north of the Tibet/Nepal border; the rupture reached the surface at the MFT (Yule et al., 2006) as evidenced by trenching through a rupture ^{14}C dated between 1610 and 1410. Kumar et al. (2010) claim that this last trench records the ~1400 Kumaon giant event, but our comparison of the ^{14}C trench ages with the historical events in Kathmandu (Table 1) furnishes a 1344 age for the Kumaon giant event (Jayangondaperumal et al., 2013) and supports the interpretation by Yule et al. (2006).

Along this cross-section (Fig. 9B), the distance between the 1505 epicenter and the dislocation line defined by Bettinelli et al. (2006) is ~100 km. The great horizontal width of the brittle, creeping rheology zone agrees with a location along the lower flat of the MHT characterized by a slight dip (as little as 5°, from Berger et al., 2004).

4.1.3. Great earthquakes in Kumaon–Garhwal (India)

The cross-section of the Kumaon region (Fig. 9C) is adapted from Srivastava and Mitra (1994), with a re-interpretation of the Lesser Himalaya from Celerier et al. (2009). According to instrumental records, the Mw ~ 6.8 1991 Uttarkashi event initiated along the lower flat of the MHT (Fig. 9C) close to the locked line (Banerjee and Burgmann, 2002) and the rupture extended along the MHT (Cotton et al., 1996) to the north of the crustal ramp, which is inferred on the regional cross-section.

The 1803 event ruptured at least an ~200 km long segment of the MHT (Ambraseys and Douglas, 2004) but did not reach the surface at the front (Kumar et al., 2006). The epicenter of the Mw ~ 8 1803 Kumaon–Garhwal earthquake has been determined from damage reports in different locations (Ambraseys and Jackson, 2003; Ambraseys and Douglas, 2004; Rajendran and Rajendran, 2005). In this paper, we follow the work of Ambraseys and Douglas (2004) because they used 33 damage sites as against 18 for Rajendran and Rajendran (2005).

The epicenter of the 1803 event (Ambraseys and Douglas, 2004) was to the north of the 1991 epicenter; and these two epicenters were separated by a north–south gap of more than 50 km. Depending on whether the MHT dips at 7° (Berger et al., 2004) or 11° (Cotton et al., 1996), there will be 6 to 10 km difference in the hypocenter depth of the two events.

Furthermore, trenches in the northwestern Himalaya (Kumahara and Jayangondaperumal, 2012) indicate either an ~1400 event more

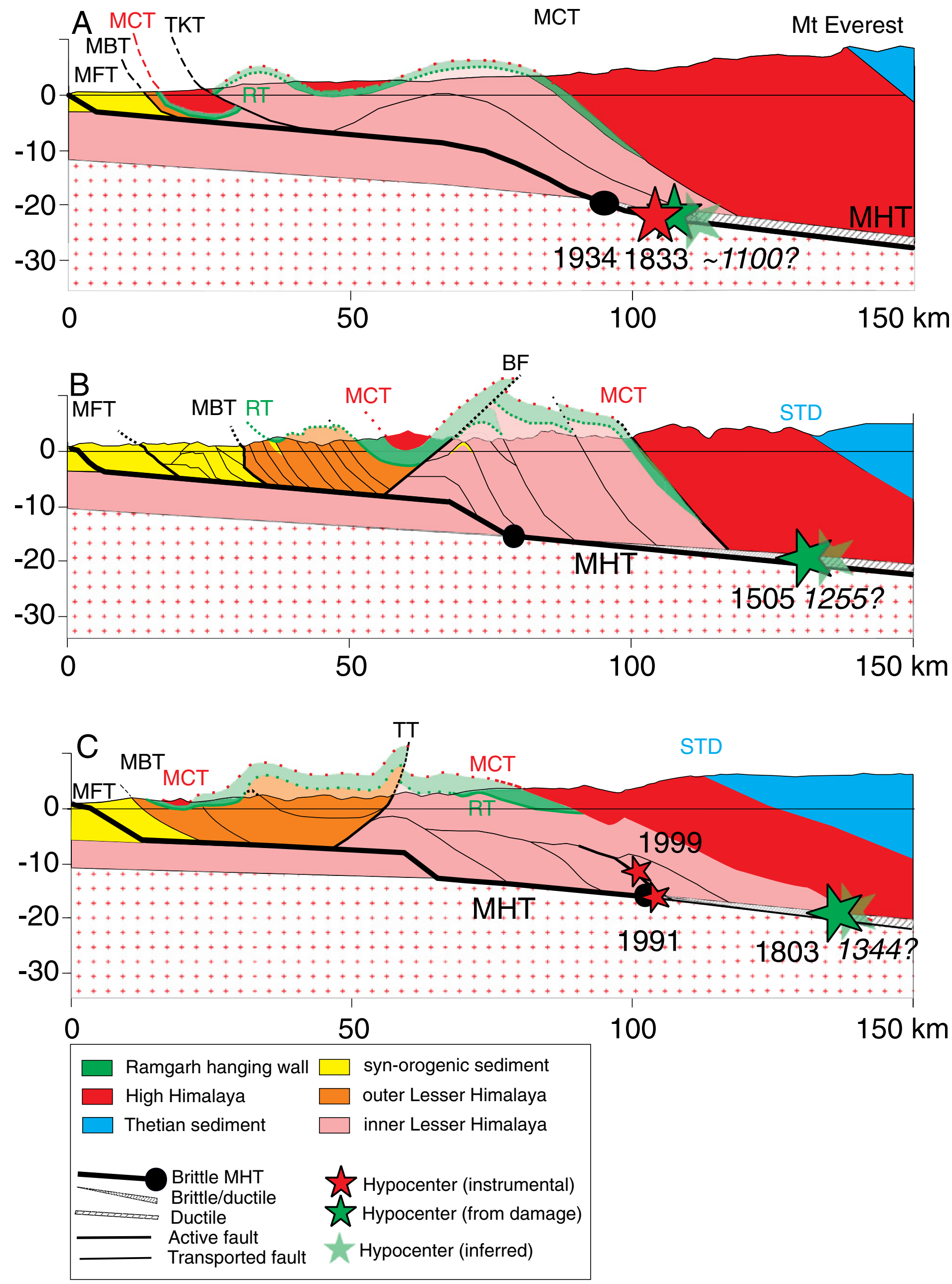

Fig. 9. Comparison of three structural cross-sections (location in Fig. 2) with rheological behavior of the MHT (Main Himalayan Thrust) and localization of historical earthquake hypocenters (see text for discussion). MCT: Main Central Thrust; MBT: Main Boundary Thrust; RT: Ramgarh Thrust (Pearson and DeCelles, 2005); MFT: Main Frontal Thrust; STD: South Tibetan Detachment; TT: Tons Thrust; BF: Bhari Ghat fault (Nakata, 1989); TKT: Tamur Khola Thrust. A) Structural section in eastern Nepal (location in Fig. 2), adapted from Schelling and Arita (1991) and Pearson and DeCelles (2005) for the Lesser Himalaya duplex, and Berger et al. (2004) for the MHT. Extent of the locked zone and tip of the dislocation (black dot) from Bettinelli et al. (2006). The rheological behavior of the MHT (Ductile, brittle/ductile transition and brittle) adapted from Berger et al. (2004). B) Structural section in western Nepal, adapted from Fuchs and Frank (1970) and Dhital and Kizaki (1987) and completed by personal field work for the Lesser Himalaya duplex, Mugnier et al. (1999) and Mugnier et al. (1992) for the Siwaliks and Berger et al. (2004) for the MHT. 1505 event from Ambraseys and Douglas (2004). Extent of the locked zone and tip of the dislocation (black dot) from Bettinelli et al. (2006). The rheological behavior of the MHT (Ductile, brittle/ductile transition and brittle) adapted from Berger et al. (2004). C) Structural section of Kumaon (adapted from Srivastava and Mitra, 1994; Celerier et al., 2009). 1803 event from Ambraseys and Douglas (2004). Extent of the locked zone and tip of the dislocation (black dot) from Banerjee and Burgmann (2002).

than 450 km in lateral extent (Kumar et al., 2006), interpreted as a giant earthquake (Feldl and Bilham, 2006), or two separate events, the eastern one being older (Jayangondaperumal et al., 2013). This eastern event, which transferred ~16 to 18 m slip to the surface (Rampur Ghanda and Lal Dhang trenches, Kumar et al., 2006), presumably occurred in 1344, supported by a correlation with the damage calendar of Kathmandu (Table 1), and must have extended eastward for Kathmandu to be badly damaged. Therefore, the displacements of the 1344 and 1803 events are different.

4.1.4. Extent of the transition zone between brittle and ductile regimes

The study of great earthquakes along three distinct cross-sections of the Himalaya (Fig. 9) confirms that the range of distribution of great earthquake hypocenters transverse-to-the arc increases as the dip of the MHT flat decreases. The horizontal (transverse-to-the-arc) extent of the brittle creeping rheology zone is narrow if located along a ramp segment (Fig. 9A) and wider, if located along a flat segment (Fig. 9B and C). The epicenters are in any case located in a zone that extends vertically no more than 6 ± 3 km (Fig. 10). This result fits with

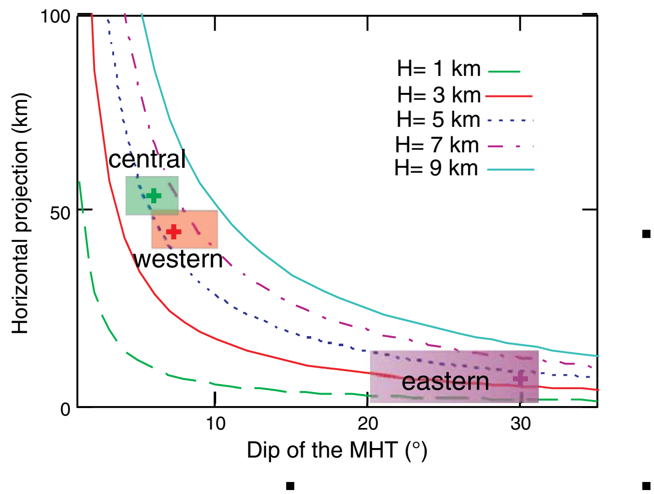

Fig. 10. Vertical extent of the brittle/ductile transition (H; incremental curves on the drawing) with respect to the dip of the MHT (X-axis) and to the horizontal projection of the distance between the locked line and the epicenter of great earthquakes (Y-axis). The dip of the MHT is estimated from Cotton et al. (1996), Berger et al. (2004) and structural cross-sections of Fig. 9. Horizontal projection of the brittle/ductile transition along the MHT is deduced from distribution of the Mw > 6 earthquakes. Purple, green, and red rectangles refer respectively to eastern, central, and western sections.

the Sibson–Scholz model (Scholz, 1998) in which the brittle/ductile transition zone typically extends to depths between 15 and 20 km. Therefore we suggest that the dispersion of the epicenters of the great earthquakes of the Himalaya is not only due to errors in locating epicenters, but that it also reflects rheological behavior.

4.2. Slip and magnitude of the great earthquakes

The cumulative slip registered along a fault is a result of both seismic and aseismic deformation (Wesnousky, 2010). Two types of aseismic (or related to events of small magnitude) behavior of a thrust zone are distinguished in the Himalaya: (1) the 2005 Kashmir earthquake was followed at depth by post-seismic deformation that did not affect the shallower part of the thrust (Jouanne et al., 2011); and (2) the vertical displacement rates evidenced by leveling along the HFT (Jackson and Bilham, 1994) seem to be consistent with a small amount of aseismic slip along the southern part of the MHT (a few mm/yr); shallow aseismic creep has nonetheless not been documented by geodesy, and even if the results of Jackson and Bilham (1994) were correct, aseismic creep would be less than 10% of the cumulative slip registered along a fault (Berger et al., 2004) and is considered negligible (Bilham et al., 2001).

Nonetheless, estimation of slip and magnitude for historical or paleo-earthquakes is an area that requires much work if we are to better understand the process of earthquake rupture (e.g. Wesnousky, 2008). Due to the complexity of the problem, in this paper, we mainly refer to the previous work carried out in the Himalaya to estimate slip and magnitude.

4.2.1. Slip and geometric characteristics of earthquakes

The geometric characteristics of earthquakes have been estimated as explained below: the minimum width of the ruptures (W) is the distance between the leading edge of the dislocation and the front of the cross-sections (Fig. 9). The length (L) is deduced from correlating the age of the ruptures in the trenches (Fig. 3 and column width in Table 1). The surface slip (S) is deduced from surface displacement evidenced in trenches (see references cited in the caption to Fig. 3). The Wells and Coppersmith (1994) relations suggest that the average surface displacement is about one-half the maximum, whereas the average subsurface displacement is smaller than the maximum surface displacement and greater than the average surface displacement. We therefore use the average surface displacement as a minimum estimate of the average subsurface slip and the maximum surface displacement as a maximum estimate of the average subsurface slip (Fig. 11A and column slip in Table 1).

For recent historical earthquakes, the relations of Kanamori (1983)—where $Mw = 2/3\log10(M0) - 6$ and $M0 = \mu LWS$ (where the elastic shear modulus μ is $3.3 \cdot 10^{10}$ N/m^2)—were used to link the seismic moment M0, deduced from isoseismal maps (Ambraseys and Douglas, 2004), to the geometric parameters. The equation is nonetheless under-constrained and the rupture geometry was chosen in order to nearly fit the calibrated VII isoseismal extents.

For the instrumentally recorded earthquakes, geometric parameters are deduced from rupture models (Cotton et al., 1996; Avouac et al., 2006; Satyabala and Bilham, 2006; Hough and Bilham, 2008).

4.2.2. Earthquake magnitudes

For historical earthquakes in this study, magnitude is deduced from isoseismal maps through the calibration performed by Ambraseys and Douglas (2004). For prehistoric events, the magnitude scale is deduced from the above estimation of geometric parameters (length, width, and slip) of the ruptures and from studies relating magnitude to

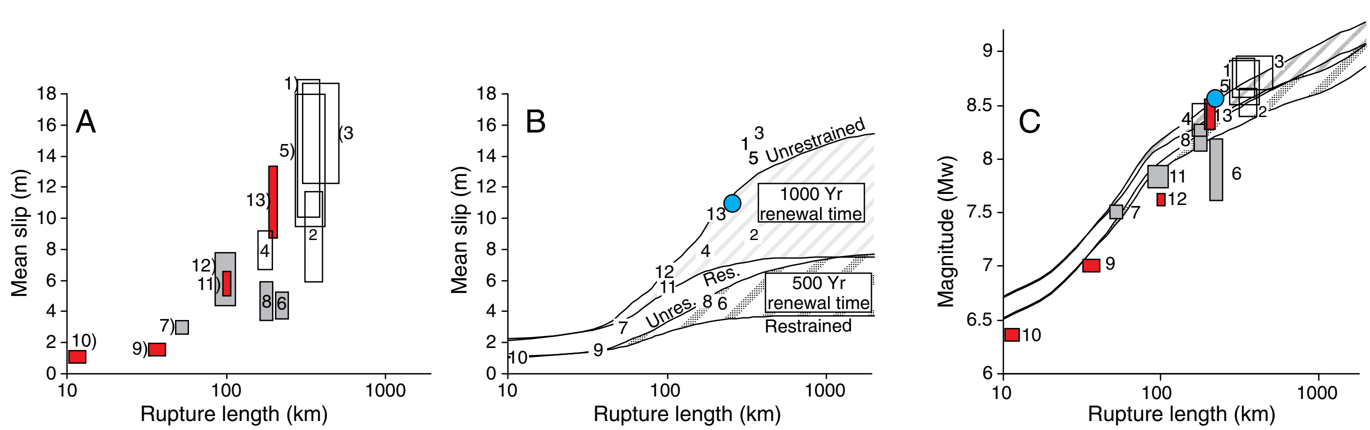

Fig. 11. Mean slip and magnitude versus rupture length for the great central Himalaya earthquakes; rectangles 1) to 10) refer to the earthquakes labeled in the left column of Table 1, and 11) to 13) refer to 2005, 1905 and 1950 events, respectively; red, gray, and white rectangles refer respectively to the instrumental, historical, and paleo-events. Blue dots refer to the discussion of the minimum estimate of the seismic hazard magnitude; A) mean slip estimate. B) Time interval necessary to renew the slip (from Feldl and Bilham, 2006). Envelopes indicate minimum slip (no plateau afterslip) and maximum slip (full strain release) for Himalayan ruptures for a renewal time interval of 500 and 1000 years. Maximum slip in medieval earthquakes 3), 1) and 5) would require a strain accumulation interval of more than 1000 yr. C) Magnitude estimate: medieval earthquakes would require a more than 8.4 magnitude, but more work is needed for earthquakes with a rupture length greater than 270 km.

the geometric parameters. The analytical work of Kanamori (1983) furnished a first approach (e.g. Lavé et al., 2005) but Feldl and Bilham (2006) have proposed a numerical modeling approach in which the Tibetan Plateau acts as a buttress that stores energy elastically over a transverse-to-the-arc width of several hundred kilometers; not every great rupture releases all the strain stored by southern Tibet and the slip depends on both the time interval between two earthquakes and the width of the rupture (Fig. 11B). Furthermore, two end-member conditions were considered in the boundary element modeling (Feldl and Bilham, 2006): in the first case, slip beneath the Himalaya is calculated assuming that no slip beneath the plateau accompanies rupture, that is, coseismic slip at the northern edge of the earthquake ceases abruptly at the southern edge of the region of aseismic slip. In the second case, the combined change in slip on the earthquake rupture and beneath the plateau is calculated, that is, the northern edge of the earthquake rupture is unrestrained and slip on the earthquake rupture is driven by strain relaxation in the southern plateau. The magnitude of the earthquake is also calculated from the size of the rupture (length and width) and the inter-seismic time interval in restrained and unrestrained boundary conditions (Fig. 1111C adapted from Feldl and Bilham, 2006).

4.3. Implications for the seismic cycle in the Himalaya

4.3.1. Variability in Himalayan earthquake ruptures

The lateral and frontal extent of a rupture along the MHT is limited by numerous rheological and geometrical conditions along the Himalayan arc, leading to various forms of ruptures (Fig. 12).

Giant and great earthquakes affecting the whole brittle MHT (Fig. 12B) nucleate somewhere between the tip of a dislocation, which is identified during the interseismic deformation, and the deeper part of the brittle creeping rheology zone (Fig. 12A), which may lie several tens of kilometers north of the tip of dislocation in the case of a flat segment.

Great earthquakes do not always cause a surface rupture such as in the 1833 event (Fig. 12C). The extent of rupture is also controlled by the location of the brittle creeping zone with respect to the crustal ramp which acts like a large-scale asperity; ruptures affecting the lower flat do not necessarily propagate southward along the ramp as exemplified by the medium-magnitude Kumaon–Garhwal 1991 event (Fig. 12D).

Nakata (1989) reports active faulting along a portion of the MCT in western Nepal in conjunction with the evolution of the Himalayan thrust wedge (Chalaron et al., 1995). Robert et al. (2011) show that this out-of-sequence component is weak, in contrast to Wobus et al. (2005) who previously suggested that the exhumation of the High Himalaya might be driven by such out-of-sequence reactivation. We suggest that this active fault branches off the brittle/ductile transition zone of the MHT (Fig. 12F) and could induce out-of-sequence earthquakes similar to the 2005 event (Avouac et al., 2006; Kondo et al., 2008) or the 1555 event (Vassallo et al., 2012) in Kashmir; in this case, the ramp ruptured during the main shock and branched off a flat (Fig. 12E), which was affected by brittle/ductile deformation (Jouanne et al., 2011). Such branching from the brittle/ductile transition zone also occurs for the roof thrust of the Lesser Himalaya duplex and seems to favor its present-day reactivation, leading to blind earthquakes (Fig. 12G) like the 1999 Chamoli event (Satyabala and Bilham, 2006).

Some out-of-sequence activity has been observed for thrusts in the brittle wedge (Mugnier et al., 2005) or back-thrusts (Nakata, 1989). Their limited offset at the surface (less than 3 m, from Mugnier et al., 2005) suggests that they are related to ruptures that affect only a part

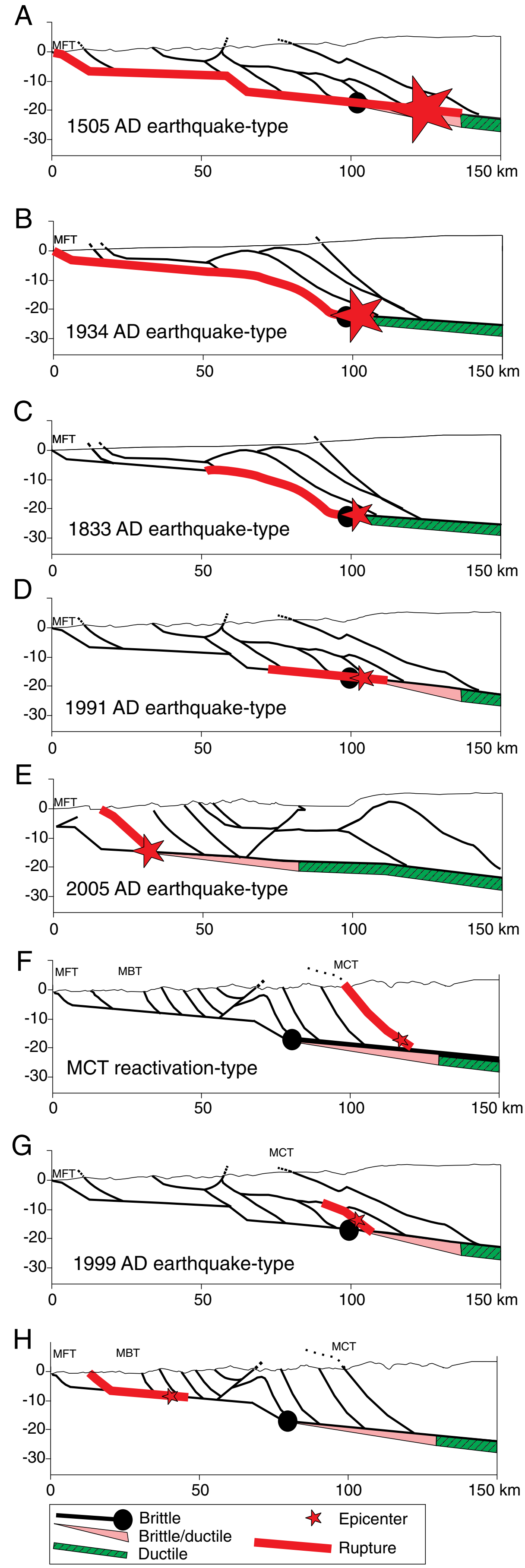

Fig. 12. Sketch of the different kinds of Himalayan ruptures. A) Giant earthquake; B) great earthquake; C) blind rupture of the ramp and upper flat; D) blind rupture of the lower flat; E) and F) reactivation to the surface of transported thrusts; G) reactivation of fault of the overlying duplex structure; H) rupture of the upper flat of the MHT with (or without) reactivation of a transported ramp.

of the brittle MHT (Fig. 12H). Ruptures that affect only a restricted portion of the brittle MHT are also evidenced from instrumental seismicity which indicates 5 < Mw < 6 earthquakes (Baranowski et al., 1984) with gently northward dipping nodal planes, like the Mw 5.5 1997 event (USGS, 2011; Thakur et al., 2012).

4.3.2. An irregular seismic cycle

We have estimated the last millennium of the evolution of the slip delivered by the great Himalayan earthquakes (Fig. 13A, B, C) by considering that every great earthquake reported in our compilation (Table 1) was of large lateral extent and affected one of the three cross-sections of the Western, Central and Eastern segments of Himalaya. The upper and lower range of the estimate for the mean sub-surface slip is discussed in Section 4.2.1. Along the eastern and western cross-sections, slip delivered episodically by the great earthquakes probably accommodates all of the ~20 m Himalayan convergence inferred for a millennium (Mugnier et al., 2004). Even in the central seismic gap of the Himalaya, where the present-day slip deficit has reached ~10 m since 1505, the slip deficit over the last millennium is negligible.

The close succession of two earthquakes in eastern Nepal (1833 and 1934 events) and in western Nepal (1255 and 1505 events), respectively, confirms a partial release of the strain stored by southern Tibet during earthquakes: for the 1934 event, the slip was more than 3 m and only 2 m convergence had accumulated since 1833, assuming an ~20 mm/yr long-term shortening rate (Mugnier et al., 2004); therefore several meters accumulated before the 1833 event but were not released by this Mw ~ 7.6 earthquake. The assumption of a short slip for the 1505 event indicates 9 m displacement with 5 m accumulated since 1255 and 4 m accumulated before 1255, but not released by the Mw > 8 1255 earthquake.

The partial strain released during an earthquake has been instrumentally measured in several oceanic subduction environments: at the Andean convergent margin, the main >10 m slip patch of the Mw 8.8 2010 earthquake occurred in an area that had already released >10 m of slip in 1960 and that was highly coupled before 2010 (Melnick et al., 2012; Moreno et al., 2012); this area appears to be the locus of high slip release and high interseismic coupling over several earthquake cycles (Melnick et al., 2009). In the Sumatra subduction zone, Konca et al. (2008) found that two earthquakes (Mw 8.4 and Mw 7.9) ruptured in 2007 within the area of the Mw 9.0 1833 event; in Japan, the Mw 8.1 2003 Tokachi-oki earthquake ruptured the same region as the Mw 8.2 1952 Tokachi-oki event (Miura et al., 2004).

In the absence of a complete release of strain during a great earthquake like the 1255 or 1833 events, we conclude that great earthquakes may occur anytime in the Himalaya.

4.3.3. How great can an earthquake be in the Himalaya?

The estimation of the greatest magnitude earthquake that can be expected in Himalaya is mainly a function of the expected slip value and size of the rupture. Numerical modeling (Feldl and Bilham, 2006) also suggests an influence of the boundary conditions during slip and the renewal time between great earthquakes.

Kumar et al. (2010) suggested that the lateral extent of the ~1400 (western India) and 1100 (eastern Himalaya) events are in the order of 900–1000 km, a distance that oversteps along-arc asperities; furthermore, slips of ~17–18 m (Lavé et al., 2005; Kumar et al., 2010) were deduced from trenching studies. Mean slip values predicted by numerical modeling (Feldl and Bilham, 2006) are smaller than the above values, even in unrestrained conditions and with a millennium time interval (Fig. 11B). This implies earthquakes of magnitudes as great as 9 and with a recurrence time greater than 1000 years (Fig. 11C adapted from Feldl and Bilham, 2006).

Nonetheless, if earthquake-related ruptures overstep an along-arc asperity, its magnitude does not increase as fast as the total rupture area (Molnar, 1987) but splits into nearly independent earthquakes (Hough and Bilham, 2008) as exemplified by the 1905 Kangra event. In the central Himalaya, at least three along-arc asperities segment the MHT at ~82°E longitude (Mugnier et al., 1999), ~85°E longitude (Mugnier et al., 2011), and ~89°E longitude (Hauck et al., 1998) in portions of 270 km along-arc length. Therefore, even for the two medieval event scenarios (Fig. 3B), the events would be split and the rupture lengths of the main shocks would be close to the rupture lengths inferred in the cluster scenario (Fig. 3C).

Assuming that (1) the along-arc asperities divide any giant slip event into 270 km segments, (2) and the mean sub-surface slip is delivered towards the north of the locked zone (unrestrained slip model) and (3) a millennium renewal time, the numerical model of Feldl and Bilham (2006) would predict a mean slip of ~11 m—a value that is not ruled out by the trenching studies (see discussion in Section 2.3)—and a magnitude of Mw 8.6 (cf. blue dot in Fig. 11). This magnitude appears to be a minimum estimate for seismic hazard in the central Himalaya.

A giant surface rupturing earthquake was observed in the far eastern Himalaya and tilting of growth strata was ascribed to the Mw ~ 8.5 historical 1950 Assam earthquake (Jayangondaperumal et al., 2011). Therefore the seismic hazard in the entire Himalaya can be calibrated at minima from the example of this last event.

Earthquakes with Mw as great as 9 cannot be ruled out in this environment, but more work has to be performed on paleo-seismologic data acquisition and rupture modeling of the events extending for more than 270 km.

The same approach could be used in other continental environments. On the northwestern side of the India–Eurasia collision, the Pamir frontal thrust is divided into segments (e.g. Arrowsmith and Strecker, 1999) that record differential absorption of plate convergence and control on earthquake ruptures. Megathrust earthquakes in the northern Chile subduction zone are controlled by the surface structures that build Andean topography (Bejar-Pizarro et al., 2013), whereas in the Andean continental back arc, inherited structures segment the locked zone (e.g. Baby et al., 1997) and out-of-sequence thrusts could reduce the width of the rupture zone (Mugnier et al., 2006). Therefore

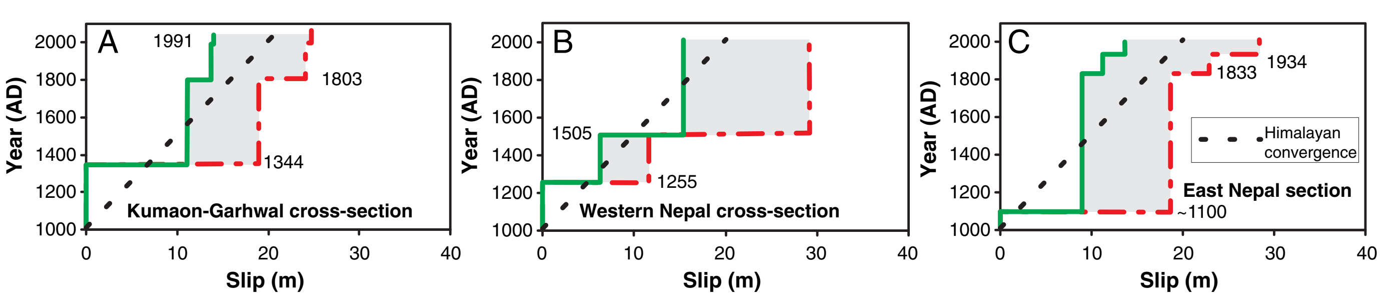

Fig. 13. A), B) and C) Sketches of the last millennium evolution of the mean sub-slip delivered by the great earthquakes respectively beneath the western, central, and eastern segments of the Himalaya (see cross sections in Fig. 9). Upper bound (red dashed and dotted line) and lower bound (green solid line) are discussed in Section 4.2.1 (see also Table 1). The episodic slip delivered is compared to the 20 mm/yr long-term shortening beneath the Himalaya (black dashed line).

the magnitude 8.7–8.9 estimation of Brooks et al. (2011), based on a rupture of the entire locked section of the continental back thrust, might have to be revised downwards slightly.

5. Conclusion

One of the major problems in understanding the seismic cycle in the Himalaya is to simultaneously take into account: (1) the medium instrumental earthquakes (6 < Mw < 7) that are occurring along gently dipping segments or along lateral ramps of the locked MHT; (2) the rather great (Mw > 7.5) historical earthquake ruptures that apparently did not reach the surface; (3) the giant paleo-earthquakes evidenced by trenching that reached the surface with great displacement (>15 m); (4) the along-arc and transverse-to-the-arc segmentations of the MHT that control the extent of ruptures in the Himalaya and split up a great earthquake into a succession of ruptures of several segments; and (5) the extent of the zone between the purely brittle and the purely ductile regime. Due to this complexity, no single method provides sufficient information to discover all the great paleo-earthquakes and to potentially evaluate seismic risk along the southern Himalayan front.

Multidisciplinary approaches promises a better understanding of earthquake dynamics and our work provides examples of the complementarity of these methods: (1) trenching is a powerful tool, but the lateral extent of a rupture is difficult to estimate, due to uncertainties in the age of the surface rupture in each trench; robust ages are obtained by comparison with the historical record and by dating large quantities of charcoal (20 ^{14}C dates were used in estimating the Marha Khola rupture at between 1020 and 1160); (2) the estimation of surface slip from trench geometry requires a detailed structural and geomorphological analysis of the surrounding site and geophysical methods (Ground Penetrating Radar and/or Electrical Resistivity Tomography) can improve estimates of fault dip; (3) detailed sedimentological studies of seismites constitute an essential tool for obtaining information in addition to trenching and historical studies (comparison between soft-sediment deformation dated in Kumaon, surface rupture dated in western Nepal and historical damage record in Kathmandu allows the determination of the 1255 event); (4) the comparison of seismological studies and damage data yields more information than a simple isoseismal map (from a combined structural and seismological analysis, the role of high-energy P-waves in dike development in the Kathmandu basin is emphasized and the epicenter of the Mw ~ 7.6 1833 earthquake is determined as being located to the NE of Kathmandu, a location that implies an overlap with the 1934 rupture); (5) segmentation of the MHT controls the extent of the ruptures and may be approached both by geodetic measurement of the inter-seismic deformation field and by geologic study of the structures related to the long-term deformation; and (6) understanding earthquake dynamics requires complex models (the 1934 earthquake released strain elastically stored in the area prior to the 1833 earthquake but not released by it).

Our compilation of great earthquakes in the central Himalaya indicates an irregular succession of seismic events. In these regions, the ~1100, 1833, and 1934 earthquakes in eastern Nepal form a succession that is neither characterized by constant displacement nor constant recurrence but accommodates all of or even more than the millennium scale Himalayan convergence. Even in the central seismic gap of the Himalaya, where the present-day slip deficit reaches ~10 m, the slip deficit at the millennium scale is negligible. The wide variety of earthquakes evidenced in the Himalaya is controlled by the along-arc segmentation of the MHT, the horizontal distribution of the transition zone between ductile and brittle deformation, and the geometry of the transported Himalayan structures.

The interpretation of the available data suggests a rather random release of seismic energy and that a great earthquake could occur anytime at all along the front of the central Himalaya. Such a result must be kept in mind for seismic hazard management planning in this densely populated area: the time since the last great historical earthquake is of no consequence, as the concept of a rather regular return time between catastrophic earthquakes is probably not relevant for the Himalaya. Furthermore, although the maximum magnitude of the historical events in the central Himalaya is 8.1, a giant earthquake of Mw ≥ 8.6 cannot be ruled out.

Acknowledgments

This work was funded by the French ANR (Paksis) and INSU (Syster) programs. A. Gajurel's stay in France was supported by a grant from Université Joseph Fourier. We thank C. Beck, and L. Audin for numerous discussions and comments on preliminary versions. R. Thiede, M. Strecker and an anonymous reviewer performed very detailed reviews. P. Miller and C. Sutcliffe copy edited the English.

References

Ader, T., Avouac, J.P., Liu-Zeng, J., Lyon-Caen, H., Bollinger, L., Galetzka, J., Genrich, J., Thomas, M., Chanard, K., Sapkota, S., Rajaure, S., Shrestha, P., Ding, L., Flouzat, M., 2012. Convergence rate across the Nepal Himalaya and interseismic coupling on the Main Himalayan Thrust: implications. J. Geophys. Res. 117, B04403. http://dx.doi.org/10.1029/2011JB009071.
Ambraseys, N.N., 1988. Engineering seismology. Earthquake Eng. Struct. Dyn. 17, 1–105.
Ambraseys, N.N., Douglas, J., 2004. Magnitude calibration of north Indian earthquakes. J. Geophys. Int. 158, 1–42.
Ambraseys, N.N., Jackson, D., 2003. A note on early earthquakes in northern India and southern Tibet. Curr. Sci. 84, 571–582.
Argand, 1924. La tectonique de l'Asie. Compte rendu du congrès géologique international (1922)Vaillant-Carmane press, Liege, Belgium (104 pp.).
Arrowsmith, J.R., Strecker, M.R., 1999. Seismotectonic range-front segmentation and mountain-belt growth in the Pamir-Alai region, Kyrgyzstan (India–Eurasia collision zone). GSA Bull. 111, 1665–1683.
Avouac, J.P., 2003. Mountain building, erosion and the seismic cycle in the Nepal Himalaya. In: Dmowska, R. (Ed.), Advances in Geophysics, 46. Elsevier, Amsterdam, pp. 1–80. http://dx.doi.org/10.1016/S0065-2687(03)46001-9.
Avouac, J.P., Bollinger, L., Lavé, J., Cattin, R., Flouzat, M., 2001. Le cycle sismique en Himalaya. C. R. Acad. Sci. 333, 513–529.
Avouac, J.-P., Ayoub, F., Leprince, S., Konca, O., Helmberger, D.V., 2006. The 2005, Mw 7.6 Kashmir earthquake: sub-pixel correlation of ASTER images and seismic waveforms analysis. Earth Planet. Sci. Lett. 249, 514–528.
Baby, P., Rochat, P., Mascle, G., Herail, G., 1997. Neogene shortening contribution to crustal thickening in the back arc of central Andes. Geology 25, 883–886.
Banerjee, P., Burgmann, R., 2002. Convergence across the northwest Himalaya from GPS measurements. Geophys. Res. Lett. 29 (13), 1652. http://dx.doi.org/10.1029/2002GL015184.
Baranowski, J., Armbruster, J., Seeber, L., Molnar, P., 1984. Focal depths and fault plane solutions of earthquakes and active tectonics of the Himalaya. J. Geophys. Res. 89, 6918–6928.
Bejar-Pizarro, M., Socquet, A., Armijo, R., Carrizo, D., Genrich, J., Simons, M., 2013. Andean structural control on interseismic coupling in the North Chile subduction zone. Nat. Geosci. 2013. http://dx.doi.org/10.1038/ngeo1802.
Benioff, H., 1938. The determination of the extent of faulting with application to the Long Beach earthquake. Bull. Seismol. Soc. Am. 28, 77–84.
Berger, A., Jouanne, F., Hassani, R., Mugnier, J.L., 2004. Modelling the spatial distribution of present-day deformation in Nepal. How cylindrical is the Main Himalayan Thrust in Nepal? Geophys. J. Int. 156, 94–112.
Bettinelli, P., Avouac, J.P., Flouzat, M., Jouanne, F., Bollinger, L., Willis, P., Chitrakar, G.R., 2006. Plate motion of India and interseismic strain in the Nepal Himalaya from GPS and DORIS measurements. J. Geod. http://dx.doi.org/10.1007//s00190-006-0030-3.
Bilham, R., 1995. Location and magnitude of the 1833 Nepal earthquake and its relation to the rupture zones of contiguous great Himalayan earthquakes. Curr. Sci. 69, 101–127.
Bilham, R., 2004. Earthquakes in India and the Himalaya: tectonics, geodesy and history. Ann. Geophys. 47, 839–855.
Bilham, R., Larson, K., Freymuller, J., Project IDYLIM members, 1997. Indo-Asian collision rates in Nepal. Nature 386, 61–64.
Bilham, R., Gaur, V.K., Molnar, P., 2001. Himalayan seismic hazard. Science 293, 1442–1444.
Brooks, B.A., Bevis, M., Whipple, K., Arrowsmith, J.R., Foster, J., Zapata, T., Kendrick, E., Minaya, E., Echalar, A., Blanco, M., Euillades, P., Sandoval, M., Smalley, R.J., 2011. Orogenic-wedge deformation and potential for great earthquakes in the central Andean backarc. Nature Geoscience 4, 380–383. http://dx.doi.org/10.1038/ngeo1143.
Campbell, A., 1833. Further particulars of the earthquake in Nepal. J. Asiat. Soc. Bengal 2, 636–639 (Misc. VI).
Celerier, J., Harrison, T.M., Webb, A.A.G., Yin, A., 2009. The Kumaun and Garwhal Lesser Himalaya, India: part 1. Structure and stratigraphy. Geol. Soc. Am. Bull. 121, 1262–1280. http://dx.doi.org/10.1130/B26344.1.
Chalaron, E., Mugnier, J.L., Mascle, G., 1995. Control of thrust tectonics in the Himalayan foothills: a view from a numerical model. Tectonophysics 248, 139–163.
Champel, B., Van Der Beek, P., Mugnier, J.L., Leturmy, P., 2002. Growth and lateral propagation of fault-related folds in the Siwaliks of western Nepal: rates, mechanisms and geomorphic signature. J. Geophys. Res. 107. http://dx.doi.org/10.1029/2001JB000578.
Chandra, U., 1992. Seismotectonics of Himalaya. Curr. Sci. 62, 40–72.

Chen, W., Molnar, P., 1977. Seismic moments of major earthquakes and the average rate of slip in central Asia. J. Geophys. Res. 82, 2945–2969.
Chitrakar, G.R., Pandey, M.R., 1986. Historical earthquakes of Nepal. Bull. Geol. Soc. Nepal 4, 7–8.
Clements, T., 1933. Notes on the fall of columns during the Long Beach Earthquake. Science 78, 100–101.
Cotton, F., Campillo, M., Deschamps, A., Rastogi, B., 1996. Rupture history and seismotectonics of the 1991 Uttarkashi, Himalayas earthquake. Tectonophysics 258, 35–51.
Dhital, M., Kizaki, K., 1987. Structural aspect of the Northern Dang, Lesser Himalaya. Bulletin of the College of Science, 45. University of the Ryukyus 159–182.
Dixit, A., Dwelly-Samant, L., Nakarmi, M., Tucker, B., Pradhanang, S., 1998. The Kathmandu Valley Earthquake Management Plan.National Society for Earthquake Technology, Nepal (37 pp. (www.preventionweb.net/english/professional/publications/v.php?id=1496)).
Dunn, J., Auden, J., Roy, S., 1939. The Bihar–Nepal Earthquake of 1934. Mem. Geol. Soc. of India, 73. Survey of India, Calcuta (391 pp.).
Feldl, N., Bilham, R., 2006. Great Himalayan earthquakes and the Tibetan plateau. Nature 444, 165–170.
Fuchs, G., Frank, W., 1970. The geology of West Nepal between the rivers Kali Gandaki and Thulo Bheri. Jahrbuch der Geologischen Bundesanstalt, Sond, 18 (Eigentümer, Wien, 103 pp.).
Gajurel, A., 2006. Etude sédimentologique et géochimique (isotopes stables) des basins syn-orogéniques de l'Himalaya du Népal (Siwaliks et basin de Kathmandu). Grenoble University (PhD thesis 301 pp.).
Hauck, M.L., Nelson, K.D., Brown, L.D., Zhao, W., Ross, A.R., 1998. Crustal structure of the Himalayan orogen at 90° east longitude from project INDEPTH deep reflection profiles. Tectonics 17, 481–500.
HMG of Nepal Ministry of Housing Physical Planning, 1993. Seismic Hazard and Risk Assessment for Nepal (Liquefaction Susceptibility Map of the Kathmandu Valley). (UNDP/UNCH3 (Habitat) Sub project NEP/88/054/21.03).
Hough, S.E., Bilham, R., 2008. Site response of the Ganges basin inferred from re-evaluated macroseismic observations from the 1897 Shillong, 1905 Kangra, and 1934 Nepal earthquakes. J. Earth Syst. Sci. 117, 773–782.
Hough, S.E., Bilham, R., Ambraseys, N., Feldl, N., 2005. Revisiting the 1897 Shillong and Kangra earthquakes in northern India: site response, Moho reflection and a triggered earthquake. Curr. Sci. 2, 1632–1638.
Huyghe, P., Mugnier, J.L., 1992. Short-cut geometry during structural inversions: competition between faulting and reactivation. Bull. Soc. Geol. Fr. 163, 691–700.
Jackson, M., Bilham, R., 1994. Constraints on Himalayan deformation inferred from vertical velocity fields in Nepal and Tibet. J. Geophys. Res. 99, 13897–13912.
Jayangondaperumal, R., Thakur, V.C., 2008. Co-seismic secondary surface fractures on southeastward extension of the rupture zone of the 2005 Kashmir earthquake. Tectonophysics 446, 61–76.
Jayangondaperumal, R., Thakur, V.C., Suresh, N., 2008. Liquefaction features of the 2005 Muzaffarabad–Kashmir earthquake and evidence of palaeoearthquakes near Jammu, Kashmir Himalaya. Curr. Sci. 95, 1071–1076.
Jayangondaperumal, R., Wesnousky, S., Chaudhari, B., 2011. Note on early to late Holocene surface faulting along the north eastern Himalayan Frontal Thrust. Bull. Seismol. Soc. Am. 101, 3060–3064. http://dx.doi.org/10.1785/0120110051.
Jayangondaperumal, R., Mugnier, J.L., Dubey, A.K., 2013. Earthquake slip estimation from the scarp geometry of Himalayan Frontal Thrust, western Himalaya: implications for seismic hazard assessment. Int. J. Earth Sci. (Geol. Rundsch.) 1–15. http://dx.doi.org/10.1007/s00531-013-0888-2.
Jouanne, F., Mugnier, J.L., Gamond, J.F., Le Fort, P., Pandey, M.R., Bollinger, L., Flouzat, M., Avouac, J.P., 2004. Current shortening across the Himalaya of Nepal. Geophys. J. Int. 157, 1–14.
Jouanne, F., Latif, M., Majid, A., Kausar, A., Pecher, A., Mugnier, J.L., 2011. Current shortening across the Himalayas: quantification of interseismic deformation in Nepal and first results of postseismic deformation in Pakistan after the 8th October earthquake. J. Geophys. Res. 116, B07401. http://dx.doi.org/10.1029/2010JB007903.
Kanamori, H., 1983. Magnitude scale and quantification of earthquakes. Tectonophysics 93, 185–199.
Kaneda, H., Nakata, T., Tsutsumi, H., Kondo, H., Sugito, N., Awata, Y., Akhtar, S.S., Majid, A., Khattak, W., Awan, A.A., Yeats, R.S., Hussain, A., Ashraf, M., Wesnousky, S.G., Kausar, A.B., 2008. Surface rupture of the 2005 Kashmir, Pakistan, earthquake and its active tectonic implications. Bull. Seismol. Soc. Am. 98, 521–557. http://dx.doi.org/10.1785/0120070073.
Konca, A.O., Avouac, J.P., Sladen, A., Meltzner, A., Sieh, K., Fang, P., Li, Z., Galetzka, J., Genrich, J., Chlieh, M., Natawidjaja, D.H., Bock, Y., Fielding, E.J., Ji, C., Helmberger, D.V., 2008. Partial rupture of a locked patch of the Sumatra megathrust during the 2007 earthquake sequence. Nature 456, 631–635. http://dx.doi.org/10.1038/nature07572.
Kondo, H., Nakata, T., Akhtar, S., Wesnousky, S., Sugito, N., Kaneda, H., Tsutsumi, H., Khan, A., Khattak, W., Kausar, A., 2008. Long recurrence interval of faulting beyond the 2005 Kashmir earthquake around the northwestern margin of the Indo-Asian collision zone. Geology 36, 731–734. http://dx.doi.org/10.1130/G25028A.
Kumahara, Y., Jayangondaperumal, Y., 2012. Paleoseismic evidence of a surface rupture along the northwestern Himalayan Frontal Thrust (HFT). Geomorphology. http://dx.doi.org/10.1016/j.geomorph.2012.09.004.
Kumar, S., Wesnousky, S.G., Rockwell, T.K., Ragona, D., Thakur, V.C., Seitz, G.G., 2001. Earthquake recurrence and rupture dynamics of Himalayan Frontal Thrust, India. Science 294, 2328–2331.
Kumar, S., Wesnousky, S., Rockwell, T.K., Briggs, R.W., Thakur, V.C., Jayangondaperumal, R., 2006. Paleoseismic evidence of great surface rupture earthquakes along the Indian Himalaya. J. Geophys. Res. 111, B03304. http://dx.doi.org/10.1029/2004JB003309.
Kumar, S., Wesnousky, S., Jayangondaperumal, R., Nakata, T., Kumahara, Y., Singh, V., 2010. Paleoseismological evidence of surface faulting along the northeastern Himalayan front, India: timing, size, and spatial extent of great earthquakes. J. Geophys. Res. 115, B12422. http://dx.doi.org/10.1029/2009JB006789 (20 pp.).
Lavé, J., Avouac, J.P., 2000. Active folding of fluviatile terraces across the Siwaliks hills, Himalayas of central Nepal, implications for Himalayan seismotectonics. J. Geophys. Res. 105, 5735–5770.
Lavé, J., Avouac, J.P., 2001. Fluvial incision and tectonic uplift across the Himalayas of Central Nepal. J. Geophys. Res. 106, 26561–26592.
Lavé, J., Yule, D., Sapkota, S., Bassant, K., Madden, C., Attal, M., Pandey, R., 2005. Evidence for a great medieval Earthquake (1100 AD) in the Central Himalayas, Nepal. Science 307, 1302–1305.
Le Fort, P., 1975. Himalayas: the collided range. Present knowledge of the continental arc. Am. J. Sci. 275, 1–44.
Levi, T., Weinberger, R., Aïfa, T., Eyal, Y., Marco, S., 2006. Injection mechanism of clay-rich sediments into dikes during earthquakes. Geochem. Geophys. Geosyst. 7 (Q12009). http://dx.doi.org/10.1029/2006GC001410.
Loveless, J., Allmendinger, R., Pritchard, M., Garroway, J., González, G., 2009. Surface cracks record long-term seismic segmentation of the Andean margin. Geology 37, 23–26. http://dx.doi.org/10.1130/G25170A.
Malik, J.N., Nakata, T., Philip, G., Suresh, N., Virdi, N.S., 2008. Active fault and paleoseismic investigation: evidence of a historical earthquake along Chandigarh Fault in the Frontal Himalayan Zone, NW India. Himal. Geol. 29, 109–117.
Malik, J.N., Sahoo, A.K., Shah, A.A., 2010. Paleoseismic evidence from trench investigation along Hajipur Fault, Himalayan Frontal Thrust. NW Himalaya: implication of the faulting pattern on landscape evolution and seismic hazard. J. Struct. Geol. 32, 350–361.
Marone, C., 1998. Laboratory-derived friction laws and their application to seismic faulting. Ann. Rev. Earth Planet. Sci. 26, 643–696.
Melnick, D., Bookhagen, B., Strecker, M., Echtler, H., 2009. Segmentation of megathrust rupture zones from fore arc deformation patterns over hundreds to millions of years, Arauco peninsula, Chile. J. Geophys. Res. 114, B01407.
Melnick, D., Moreno, M., Cisternas, M., Tassara, A., 2012. Darwin seismic gap closed by the 2010 Maule earthquake. Andean Geol. 39 (3), 558–563.
Miura, S., Suwa, Y., Hasegawa, A., Nishimura, T., 2004. The 2003 M8.0 Tokachi-Oki earthquake — how much has the great event paid back slip debts? Geophys. Res. Lett. 31, L05613. http://dx.doi.org/10.1029/2003GL019021.
Molnar, P., 1987. The distribution of intensity associated with the 1905 Kangra earthquake and bounds on the extent of the rupture zone. J. Geol. Soc. India 29, 221–229.
Molnar, P., Lyon-Caen, H., 1988. Some simple physical aspects of the support, structure, and evolution of mountain belts. Processes in Continental Lithospheric Deformation. Geol. Assoc. Can. Spec. Pap., 218, pp. 179–207.
Moreno, M., Melnick, D., Rosenau, M., Baez, J., Klotz, J., Oncken, O., Tassara, A., Chen, J., Bataille, K., Bevis, M., Socquet, A., Bolte, J., Vigny, C., Brooks, B., Ryder, I., Grund, V., Smalley, B., Carrizo, D., Bartsch, M., Hase, H., 2012. Toward understanding tectonic control on the Mw 8.8 2010 Maule Chile earthquake. Earth Planet. Sci. Lett. 321–322, 152–165.
Mugnier, J.L., Huyghe, P., 2006. The Ganges basin geometry records a pre-15 Ma isostatic rebound of Himalaya. Geology 34, 445–448.
Mugnier, J.L., Mascle, G., Faucher, T., 1992. La structure des Siwaliks de l'Ouest Népal: un prisme d'accrétion intracontinental. Bull. Soc. Geol. Fr. 163, 585–595.
Mugnier, J.L., Leturmy, P., Mascle, G., Huyghe, P., Chalaron, E., Vidal, G., Husson, L., Delcaillau, B., 1999. The Siwaliks of Western Nepal: I — geometry and kinematics. J. Asian Earth Sci. 17, 629–642.
Mugnier, J.L., Huyghe, P., Leturmy, P., Jouanne, F., 2004. Episodicity and rates of thrust sheet motion in Himalaya (Western Nepal). In: McClay (Ed.), Thrust Tectonics and Hydrocarbon Systems. A. A. P. G. Mem, 82, pp. 91–114.
Mugnier, J.L., Huyghe, P., Gajurel, A.P., Becel, D., 2005. Frontal and piggy-back seismic ruptures in the external thrust belt of western Nepal. J. Asian Earth Sci. 25, 707–717.
Mugnier, J.L., Becel, D., Granjeon, D., 2006. Active tectonics in the Subandean belt inferred from the morphology of the Rio Pilcomayo. In: Willett, S.D., Hovius, N., Brandon, M.T., Fisher, D. (Eds.), Tectonics, Climate and Landscape Evolution. Geol. Soc. Am. Spec. Publ., 398, pp. 353–369.
Mugnier, J.L., Huyghe, P., Gajurel, A., Upreti, B., Jouanne, F., 2011. Seismites in the Kathmandu basin and seismic hazard. Tectonophysics 509, 33–49. http://dx.doi.org/10.1016/j.tecto.2011.05.012.
Nakata, T., 1989. Active faults of the Himalayas of India and Nepal. Geol. Soc. Am. Spec. Pap. 232, 243–264.
Nakata, T., Kumura, K., Rockwell, T., 1998. First successful paleoseismic trench study on active faults in the Himalayas. Proceedings of AGU 1998 fall meeting. Eos, Transactions AGU, 79, p. 45.
Obermeier, S., 1996. Using liquefaction-induced features for paleoseismic analysis. In: McCalpin, J. (Ed.), Paleosismology. International Geophysics Series, 62, pp. 331–396.
Obermeier, S., Pond, E., Olson, S., Green, R., 2002. Paleoliquefaction studies in continental settings. Geol. Soc. Am. Spec. Pap. 359, 13–27.
Oldham, T., 1883. A catalogue of Indian earthquakes from the earliest time to the end of A.D. 1869. Mem. Geol. Surv. India 19, 163–215.
Pandey, M.R., Molnar, P., 1988. The distribution of intensity of the Bihar–Nepal earthquake of 15 January 1934 and bounds on the extent of the rupture zone. J. Geol. Soc. Nepal 5, 22–44.
Pandey, M.R., Tandukar, R.P., Avouac, J.P., Lavé, J., Massot, J.P., 1995. Evidence for recent interseismic strain accumulation on a mid-crustal ramp in the Central Himalaya of Nepal. Geophys. Res. Lett. 22, 751–758.
Pandey, M.R., Tandukar, R.P., Avouac, J.P., Vergne, J., Héritier, Th., 1999. Characteristics of seismicity of Nepal and their seismotectonic implications. J. Asian Earth Sci. 17, 703–712.

Pant, M.R., 2002. A step toward a historical seismicity of Nepal. Adarsa 2, 29–60.
Pearson, O.N., DeCelles, P.G., 2005. Structural geology and regional tectonic significance of the Ramgarh thrust, Himalayan fold-thrust belt of Nepal. Tectonics 24, TC4008.
Perfettini, H., Avouac, J.P., 2004. Postseismic relaxation driven by brittle creep: a possible mechanism to reconcile geodetic measurements and the decay rate of aftershocks, application to the Chi-Chi earthquake, Taiwan. J. Geophys. Res. 109, B02304. http://dx.doi.org/10.1029/2003JB002488.
Rajendran, C.P., Rajendran, K., 2005. The status of central seismic gap: a perspective based on the spatial and temporal aspects of the large Himalayan earthquakes. Tectonophysics 395, 19–39.
Rajendran, K., Rajendran, C.P., 2011. Revisiting the earthquake sources in the Himalaya: perspectives on past seismicity. Tectonophysics 504, 75–88.
Rana, B.J.B., 1935. Nepal Ko Maha Bhukampa.Jorganesh Press.
Rastogi, B., Chadha, R., 1995. Intensity and isoseismals of Uttarkashi earthquake of October, 1991. In: Gupta, H.K., Gupta, G.D. (Eds.), Uttarkashi Earthquake. Geological Society of India, Memoir, 30, pp. 19–24.
Reimer, P.J., Baillie, M.G.L., Bard, E., Bayliss, A., Beck, J.W., Bertrand, C.J.H., Blackwell, P.G., Buck, C.E., Burr, G.S., Cutler, K.B., Damon, P.E., Edwards, R.L., Fairbanks, R.G., Friedrich, M., Guilderson, T.P., Hogg, A.G., Hughen, K.A., Kromer, B., McCormac, G., Manning, S., Ramsey, C., Reimer, R.W., Remmele, S., Southon, J.R., Stuiver, M., Talamo, S., Taylor, F.W., Van der Plicht, J., Weyhenmeyer, C.E., 2004. IntCal04 terrestrial radiocarbon age calibration, 0–26 cal kyr BP. Radiocarbon 46, 1029–1058.
Robert, X., van der Beek, P.A., Braun, J., Perry, C.M., Mugnier, J.L., 2011. Control of detachment geometry on lateral variations in exhumation rates in the Himalaya: insights from low-temperature thermochronology and numerical modeling. J. Geophys. Res. 116, B05202. http://dx.doi.org/10.1029/2010JB007893 (22 pp.).
Sapkota, S., 2011. Rupture de surface du séisme de Bihar–Népal 1934: implications pour l'aléa sismique en Himalaya du Népal. Institut de Physique du Globe Paris (PhD thesis 281 pp.).
Sapkota, S., Bollinger, L., Klinger, Y., Tapponnier, P., Gaudemer, Y., Tiwari, D., 2013. Primary surface ruptures of the great Himalayan earthquakes in 1934 and 1255. Nat. Geosci. 6, 71–76. http://dx.doi.org/10.1038/ngeo1669.
Satyabala, S., Bilham, R., 2006. Surface deformation and surface slip of the March 199 Mw = 6.4 west Himalayan Chamoli earthquake from InSAR analysis. Geophys. Res. Lett. L23305. http://dx.doi.org/10.1029/2006GL027422.
Schelling, D., Arita, K., 1991. Thrust tectonics, crustal shortening, and the structure of the far-eastern Nepal Himalaya. Tectonics 10, 851–862.
Scholz, C.H., 1998. Earthquakes and friction laws. Nature 391, 37–42.
Schulte-Pelkum, V., Monsalve, G., Sheehan, A., Pandey, M.R., Sapkota, S., Bilham, R., Wu, F., 2005. Imaging the Indian subcontinent beneath the Himalaya. Nature 435, 1222–1225.
Seeber, L., Armburster, J., 1981. Great detachment earthquakes along the Himalayan arc and long term forecast. In: Sibson, D.W., Richards, P.G. (Eds.), Earthquake Prediction: An International Review. Maurice Ewing Series, 4. Amer. Geophysical Union, Washington D.C., pp. 259–277.
Shibazaki, B., Tanaka, H., Horikawa, H., et al., 2002. Modeling slip processes at the deeper part of the seismogenic zone using a constitutive law combining friction and flow laws. Conference: International Symposium on Slip and Flow Processes in and below the Seismogenic Region, Sendai Japon. November 05–08, 2001. Earth, Planets and Space, 54, pp. 1211–1218.
Sibson, R., 1986. Earthquakes and rock deformation in crustal fault zone. Annu. Rev. Earth Planet. Sci. 14, 149–175.
Srivastava, P., Mitra, G., 1994. Thrust geometries and deep structure of the outer and lesser Himalayas, Kumaon of the Himalayan fold-and-thrust belt. Tectonics 13, 89–109.
Stein, S., Wysession, M., 2003. An Introduction to Seismology, Earthquakes, and Earth Structures. Blackwell Publishing Ltd., Oxford, UK (498 pp.).
Stuiver, M., Reimer, P.J., Bard, E., Beck, J.W., Burr, G.S., Hughen, K.A., Kromer, B., McCormac, F.G., v. d. Plicht, J., Spurk, M., 1998. INTCAL98 radiocarbon age calibration 24,000–0 cal BP. Radiocarbon 40, 1041–1083.
Szeliga, W., Hough, S.E., Martin, S., Bilham, R., 2010. Intensity, magnitude, location, and attenuation in India for felt earthquakes since 1762. Bull. Seismol. Soc. Am. 100, 570–584.
Thakur, V.C., Mahajan, A.K., Gupta, V., 2012. Seismotectonics of 18 September 2011 Sikkim earthquake: a component of transcurrent deformation in eastern Himalaya. Himal. Geol. 33, 89–96.
Thapa, G.S., 1997. In: Department of Mines and Geology (Ed.), Microseismic Epicenter Map of Nepal Himalaya and Adjoining Region (Kathmandu, Nepal).
Upreti, B.N., et al., 2000. The latest active faulting in Southeast Nepal. Proceedings Active Fault Research for the New Millenium, Hokudan Int. Symp. and Sch. on Active Faulting, Awaji Island, Hyogo, Japan.
Upreti, B., Kumahara, Y., Nakata, T., 2008. Evidence of two large seismic gaps in Nepal Himalaya: potential for future mega earthquakes. 33rd International Geological Congress, Oslo. http://www.cprm.gov.br/33IGC/1260752.html.
USGS, 2011. Magnitude 6.9 — India–Nepal Border Region 2011 September 18 12:40:48 UTC. http://earthquake.usgs.gov/earthquakes/eqinthenews/2011/usc0005wg6/#maps.
Vassallo, R., Vignon, V., Mugnier, J.-L., Jayangondaperumal, R., Srivastava, P., Malik, M.M., Mouchené, M., Jouanne, F., 2012. A future big one in the Himalayan North-West syntax? European Geosciences Union General Assembly 2012,Vienna, Austria 22–27 April 2012.
Wells, D., Coppersmith, K., 1994. New empirical relationships among magnitude, rupture length, rupture width, rupture area, and surface displacement. Bull. Seismol. Soc. Am. 84, 974–1002.
Wesnousky, S.G., 2008. Displacement and geometrical characteristics of earthquake surface ruptures: issues and implications for seismic hazard analysis and the process of earthquake rupture. Bull. Seismol. Soc. Am. 98, 1609–1632.
Wesnousky, S.G., 2010. Biases in the estimation of earthquake recurrence and seismic hazard from geologic data. Bull. Seismol. Soc. Am. 100, 2287–2292.
Wobus, C.W., Heimsath, A., Whipple, K.X., Hodges, K.V., 2005. Active out-of-sequence thrust faulting in the central Nepalese Himalaya. Nature 434, 1008–1011.
Yoshida, M., Igarashi, Y., 1984. Neogene to Quaternary lacustrine sediments in the Kathmandu Valley, Nepal. J. Nepal Geol. Soc. 4, 73–100.
Yule, D., Dawson, S., Lave, J., Sapkota, S., Tiwari, D., 2006. Possible evidence for surface rupture of the Main Frontal Thrust during the great 1505 Himalayan earthquake, Far-Western Nepal. EOS Trans. AGU)52 (Fall Meet. Suppl., Abstract S33C-05).
Zhang, P.Z., Shen, Z., Wang, M., Gan, W., Bürgmann, R., Molnar, P., Wang, Q., Niu, Z., Sun, J., Wu, J., Hanrong, S., Xinzhao, Y., 2004. Continuous deformation of the Tibetan Plateau from global positioning system data. Geology 32, 809–812. http://dx.doi.org/10.1130/G20554.1.
Zhao, W., Nelson, K.D., project INDEPTH Team, 1993. Deep seismic reflection evidence for continental underthrusting beneath southern Tibet. Nature 366, 55–559.